From Department of Neurobiology, Care Sciences and Society
Karolinska Institutet, Stockholm, Sweden

THE AGING FRONTAL LOBE IN HEALTH AND DISEASE

A structural magnetic resonance imaging study

Olof Lindberg

Stockholm 2012

Published by Karolinska Institutet. Printed by [US-AB universitetsservice]

ISBN 978-91-7457-695-5

In memory of my father

Carl-Erik Lindberg


SWEDISH
brain
POWER

PREFACE

Dear reader, on the front of this thesis I am proud to present my own brain! According to Erasistratus, a Greek neuroanatomist who lived 310-250 B.C.E. in Alexandria, intelligence may be reflected in the complexity of the convolutions of the brain. I am a great fan of this hypothesis, since attempting to divide my own frontal lobe into the three main gyri, particularly on the right side, has caused me no end of trouble. Contrary to most people, my superior frontal gyrus seems to grow sideways, rather than parallel to the hemispheric fissure. This complexity of the surface of my brain, I hope, shall at one point or two be reflected in convincing theories and interesting thoughts in this thesis, which thus should lend support to Erasistratus´ theory, that an owner of such a complex brain indeed must be an intelligent person.

If you have half as much fun reading this work, as I had writing it, I will consider it to be a great success!

Sincerely

Olof Lindberg.

ABSTRACT

Cortical and subcortical regions of the brain decrease in volume in normal as well as pathological aging. Previous studies indicate that certain parts of the brain, like the prefrontal cortex, may be particularly vulnerable to age-related processes which are manifested by significant volume loss in this region. Cortical volume loss may be further enhanced by different kinds of pathology in the brain.

The purpose of this study was to further investigate regional volumetric changes of the frontal lobe in normal aging and in aging patients with dementia.

In study I-III patients with frontotemporal lobar degeneration (FTLD), Alzheimer's disease (AD) and healthy controls are investigated. Cortical atrophy is related to clinical symptoms (study I), discussed in relation to gross morphology and cytoarchitecture (study II), and compared with the atrophy in the hippocampus (study III).

In study IV a large number of normal elderly participants are investigated. Age-related volume loss in the limbic system (the dorsal anterior cingulate cortex and the hippocampus) is compared with atrophy of a region of the prefrontal cortex (the orbitofrontal cortex).

Volumetric data of frontal and temporal cortical regions and the hippocampus was acquired by manual delineation on structural magnetic resonance images.

Results of study I and III reveal that the clinical symptoms displayed by the subtypes of FTLD are commonly reflected in a specific pattern of atrophy in frontotemporal cortices as well as in the hippocampus. Study II suggests that the surface morphology of sulci and gyri may be unreliable landmarks for cyto-architectonic regions of the frontal cortex. Study IV finally indicates that a common characteristic of limbic regions may be that age-related volume loss is delayed in comparison to regions of the prefrontal cortex. Results also suggest that the dorsal anterior cingulate is more resistant to age-related volume loss than hippocampus, which implies that age-related volume loss occurs at different rates for different regions also within the limbic system.

SVENSK SAMMANFATTNING

Kortikala och subkortikala hjärnregioner minskar i volym både genom sjukdom och vid normalt åldrande. Tidigare studier har visat att vissa hjärnregioner uppvisare större åldersrelaterad eller sjukdomsrelaterad volymsförlust än andra. Syftet med föreliggande studie är att ytterligare kartlägga regionala volymsförluster i hjärnans frontallob vid friskt och sjukt åldrande.

I studie I-III undersöktes volymsförluster i frontala och temporala delar av hjärnan hos patienter med olika varianter av pannlobs demens och Alzheimers demens. I **studie I** studerades sambandet mellan atrofi i kortikala och subkortikala regioner och kliniska symptom som uppvisas av patienter med pannlobsdemens. I **studie II** jämfördes volymdata för anatomiskt definierade gyri i frontalloben med volymdata som kalkylerar medelvärdet för hur mycket gråsubstans det finns i samma gyri.

Studie III jämfördes kortikal atrofi med hippocampal atrofisk deformering i de tidigare studerade patienterna med pannlobsdemens samt i patienter med Alzheimers demens.

I **studie IV** slutligen jämfördes volymen för två regioner i limbiska systemet (dorsala anteriora cingulate gyrus och hippocampus) med volymen för en prefrontal region (orbitofrontala hjärnbarken) hos 505 deltagare i SNAC-Kungsholmsprojektet mellan 60 till 97 års ålder.

Resultaten av **studie I** visade att de specifika symptom som uppvisas hos de tre kategorierna av pannlobsdemens kan relateras till tre olika mönster av kortikal atrofi. Resultaten tyder vidare på att dessa mönster reflekterar degenerering av specifika funktionella nätverk i hjärnan som i sin tur är av avgörande betydelse för de emotionella eller kognitiva processer som uppvisar störning vid de olika formerna av pannlobsdemens.

Resultaten av **studie II** indikerade att ett kalkylerat medelvärde för hur mycket gråsubstans det finns inom ett kortikalt område kan vara en känsligare indikator för kortikal degenerering än den totala volymen för ett specifikt frontal gyrus. Sannolikt skapade den anatomiska variabiliteten av kortikala gyri en varians i volymdata som inte var relaterad till ”tillståndet” i det undersökta området utan som snarare kan förklaras med anatomisk variabilitet mellan individer.

Studie III visade att de tre karaktäristiska mönster av kortikal atrofi som hittades i de tre varianterna av pannlobsdemens också motsvaras av tre mönster av atrofisk deformering av hippocampus. Ett gemensamt drag hos samtliga patienter med pannlobsdemens var att huvudet på hippocampus var proportionellt mera atrofiskt eller lika atrofiskt som kroppen och svansen på strukturen. Detta var en avgörande skillnad i jämförelse med patienter som lider av Alzheimers sjukdom som uppvisade mera deformering i kroppen än i huvudet och svansen.

Studie IV visade att två regioner i det limbiska systemet (hippocampus och dorsala anteriora cingulate gyrus) sannolikt har en fördröjd åldersrelaterad volymsförlust jämfört med en region i prefrontala hjärnbarken (orbitofrontala hjärnbarken). Skillnaden i volymsförlust i båda limbiska regionerna var ringa när man jämförde 60-, 66- och 72-åriga deltagare. Skillnaden mellan 72-, 78-, 83- och 90-åringar indikerade att volymsförlusten i hippocampus sannolikt ökar efter 72 års ålder, medan den ökade

något men var fortfarande ringa i anterior cingulate gyrus. Orbitala hjärnbarken visade ett motsatt mönster där de största skillnaderna mellan åldersgrupper hittades i jämförelsen mellan 60-, 66- och 72-åringar.

Sammantaget indikerade föreliggande studie att kortikala och subkortikala regioner i hjärnan minskar i volym både vid åldrande och vid patologiska neurodegenerativa sjukdomar. Studien visar vidare att en mängd faktorer påverkar graden och hastigheten hos sådan degenerering. Till exempel kan graden av komplexitet i cellstrukturen i en region av hjärnbarken, dess anatomiska förbindelser, typ av patologi hos patienten eller personens ålder vara avgörande faktorer för graden och hastigheten av regional volym förlust i hjärnan.

LIST OF PUBLICATIONS

I. **Cortical Morphometric Subclassification of Frontotemporal Lobar Degeneration**

Olof Lindberg, Per Östberg, Bram Zandbelt, Johanna Öberg, Yi Zhang, Lisa Botes, Christian Andersen, Nenad Bogdanović, Lars-Olof Wahlund

AJNR Am J Neuroradiol 2009;30:1233–39.

II. **A Comparison Between Volumetric Data Generated by Voxel-Based Morphometry and Manual Parcellation of Multimodal Regions of the Frontal Lobe**

Olof Lindberg, Amir Manzouri, Eric Westman, Lars-Olof Wahlund.

AJNR Am J Neuroradiol 2012;33: In press.

III. **Hippocampal Shape Analysis in Alzheimer's Disease and Frontotemporal Lobar Degeneration Subtypes**

Olof Lindberg, Mark Walterfang, Jeffrey C.L. Looi, Nikolai Malykhin, Per Östberg, Bram Zandbelt , Martin Styner, Beatriz Paniagua, Dennis Velakoulis, Eva Örndahl, Lars-Olof Wahlund

J Alzheimers Dis 2012;29:1–11: In press.

IV. **Selective preservation of the grey matter in the dorsal part of the anterior cingulate cortex at old and very old age**

Olof Lindberg, Carl-Henrik Ehrenkrona, Linnea Engström, Yi Zhang, Eva Örndahl, Erika Jonsson Laukka, Grégoria Kalpouzos, Lars-Olof Wahlund

Manuscript.

CONTENTS

LIST OF ABBREVIATIONS

3D	Three dimensional
ACC	Anterior cingulate cortex
AC-PC	Anterior-posterior commisure
AD	Alzheimer´s disease
ANOVA	Analysis of variance
BA	Brodmann area
BET	Brain extraction tool
BVT	Brain-Voyager Tutor
CA1	Corno ammonis 1
CA 2	Corno ammonis 2
CA 3	Corno ammonis 3
CA 4	Corno ammonis 4
CSF	Cerebrospinal fluid
DACC	Dorsal anterior cingulate cortex
DLPC	Dorsolateral prefrontal cortex
DLPG	Dorsolateral prefrontal gyrus
DSM IV	Diagnostic and statistical Manual of Mental Disorders IV
EC	Entorhinal cortex
FDR	False discovery rate
fMRI	Functional magnetic resonance imaging
FSL	FMRIB Software Library
FTD	Frontotemporal dementia
FTLD	Frontotemporal lobar degeneration
GM	Grey matter
HB	Hippocampal body
HC	Hippocampus (Study II and III)
HIPP	Hippocampus (Study I)
HT	Hippocampal tail
ICC	Intraclass correlation
ICD-10	International Classification of mental disorders 10 revision
ICV	Intracranial volume
IFG	Inferior frontal gyrus
M	Motor cortex
MFG	Middle frontal gyrus
MM	Manual methods
MMSE	Mini-Mental State Examination
MRI	Magnetic resonance imaging
MRIs	Magnetic resonance images
OFC	Orbitofrontal cortex (Study II and IV)
ORB	Orbitofrontal cortex (Study I)
PFC	Prefrontal cortex
PLS-DA	Partial least-square discriminant analysis

PMC	Premotor cortex
PNFA	Progressive nonfluent aphasia
r	Pearson´s product moment correlation coefficient
R	Right side
RACC	Rostral anterior cingulate cortex
RF	Radio frequency
SCI	Subjective cognitive complaint
SD	Semantic dementia
SDL	Semantic dementia with predominantly left side atrophy
SDR	Semantic dementia with predominantly right side atrophy
SFG	Superior frontal gyrus
SMPC	Subcallosal medial prefrontal cortex
SNAC-K	Swedish National study of Aging and Care in Kungsholmen
SPHARM-pdm	Shape analysis tool using spherical harmonics
TEMP	Temporal pole
VBM	Voxel-based morphometry
WHO	World Health Organization
VIP	Variable of importance
VLS	Volume of structure

1 INTRODUCTION

The brain undergoes a constant structural change from birth to old age (Fjell and Walhovd, 2010; Shaw et al., 2008). Indirect evidence for such changes at microscopic level may for example be found in the reduction or increase of the volume of cortical regions (Raz et al., 2004; Shaw et al., 2008; Tisserand et al., 2002), which can be investigated by measuring volumes on structural magnetic resonance images (MRIs). Numerous studies have shown that cortical and subcortical structures change in volume both during development (Shaw et al., 2008; Westlye et al., 2010b) and in aging (Raz et al., 2005; Tisserand et al., 2002; Walhovd et al., 2011). The frontal lobe and in particular the prefrontal cortex (PFC) may be particularly vulnerable in aging, which is manifested by more age-related volume loss in this part of the brain than in others (McGinnis et al., 2011; Raz et al., 2004; Tisserand et al., 2002). Regional brain volume loss may also be induced by pathology. In different variants of dementia such as Alzheimer's disease (AD) or frontotemporal lobar degeneration (FTLD), brain volume loss is commonly more severe than that caused by aging (Whitwell and Jack, 2005).

Volumetric changes both in normal and pathological aging have been extensively researched during the last two decades. Advances in the neuroimaging field have however provided new challenges and new research questions, concerning the relation between volume loss and properties such as the anatomical connections between brain regions, the cortical cell structures or the integrity of sub-cortical white matter. Functional magnetic resonance imaging (fMRI) acquired at resting state has provided new evidence for how clusters of cortical regions work together in different brain networks (Vincent et al., 2008). Recent studies indicate that brain pathology primarily progresses through the anatomical connections of such networks (Rönnback et al., 2011). It has furthermore been demonstrated that regional brain volume loss in dementia also occurs in a network-specific fashion and that different networks are targeted in different neurodegenerative diseases (Seeley et al., 2009).

Diffusion tensor MRI is another technique that has provided new possibilities to investigate age-related and pathological processes in the brain. By this method the white matter tracts that connect different regions in cortical networks can be investigated in great detail (Agosta et al., 2011; Catani et al., 2002; Thiebaut de Schotten et al., 2011).

Furthermore the constant improvement of several softwares that can obtain regional volume and cortical thickness automatically has increased our knowledge about how regional volumes in the cortex change, both during development and in old age, as well as in disease (Fischl et al., 2008; Shaw et al., 2008; Sowell et al., 2001; Walhovd et al., 2011; Westlye et al., 2010a; Westlye et al., 2010b).

Automated techniques for the analysis of histological sections have also improved our knowledge about the relationship between gross-morphological appearances of the cortex and the underlying cytoarchitectonic cell structure (Schleicher et al., 1986; Schleicher and Zilles, 1990).

Important insights gained from recent volumetric studies reveal that the cell structure of the cortex (Shaw et al., 2008) and the connectivity of cortical regions (Seeley et al.,

2009) or cortical systems (Grieve et al., 2005) may all be factors that influence the rate of age- or pathology-related brain volume decline.

The aim of the present study is to investigate regional loss of brain volume in the aging frontal lobe by considering the factors mentioned above. Volume loss is thus considered in relation to clinical symptoms (study I), gross morphology of the cortical surface (study II), and one cortical system (study IV). In study III a comparison between cortical and subcortical patterns of atrophy is made by comparing the patterns of atrophy in cortex with the atrophic deformation of hippocampus in subtypes of FTLD and AD. A final aim of the thesis is to discuss how the progression of atrophy in neurodegenerative disease may partly be determined by the anatomical connectivity of regions involved in a pathological process. This will be discussed by unpublished data obtained from the cohort investigated in study I, II, and III.

Thus in this thesis the frontal lobe has to be considered at several different structural levels. These will be reviewed in section (3.1-3.2.2). The characteristic clinical symptoms in FTLD that are discussed in study I are reviewed in section (4.3). Previous studies on how atrophy progresses through known anatomical connections will be discussed in section (4.5).

2 IMAGING THE BRAIN

2.1 STRUCTURAL MAGNETIC RESONANCE IMAGING

Magnetic resonance imaging (MRI) is a powerful tool to visualize the tissue of the brain (Tanev et al., 2011). MRI utilizes the magnetic properties of the hydrogen atoms to create images of the soft tissue of the brain or other organs of the body (McRobbie et al., 2005). The hydrogen atom has a nucleus (one proton) and one "moon" (one electron). The hydrogen nucleus, which is a magnetic dipole because of the protons intrinsic spin, aligns parallel or anti-parallell to the external magnetic field. In the MRI-scanner hydrogen nuclei are thus aligned parallel or anti-parallel to the main magnetic field of the scanner (denoted the z-direction). A small majority of the protons will be aligned in the lower energy state (which is parallel to the external magnetic field) is giving rise to a net magnetization in the tissue. To measure the magnetization in a tissue the alignment of the nuclei has to be knocked out by radio frequency pulses (RF) (McRobbie et al., 2005). When doing so the net magnetization can be rotated perpendicular to the main magnetic field of the scanner (the z-plane). When the RF pulse stops the magnetization falls back into the equilibrium position along the z-direction which releases energy that can be recorded by the MRI-scanner. The time required for the protons to realign with the scanner's main field (called relaxation time) is different in different kinds of tissue. The relaxation time is longest in fluids, shorter in water-based tissue, and shortest in fat-based tissue (McRobbie et al., 2005). This difference in relaxation time is the fundamental mechanism by which contrast between different kinds of soft tissue can be obtained in MRI. The MRI technique can produce a wide range of contrasts by adjusting the timing of the RF pulses and the signal acquisition (McRobbie et al., 2005). This makes this technique particularly useful for imaging the brain, making it possible to visualize the anatomy of soft tissue in great detail. Certain sequences employed in MRI allow for the collection of high resolution three dimensional (3D) datasets which are very useful for analyzing the structural characteristics of the brain.

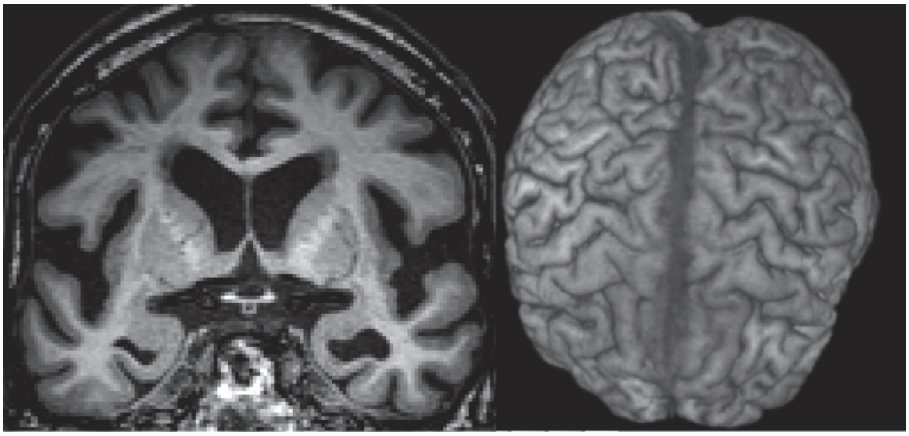

Figure 1
To the left the coronal view of the brain imaged in a 3D sequence by a MR-scanner. To the right the surface of the same brain is reconstructed on basis of the scan to the left in the software MRIcro (Version 1.37; Roden and Brett, 2000).

2.2 MEASURING VOLUMES ON MRI

Over the last ten years, numerous methods have been developed for measuring regional volumes of the brain on structural MRIs, (e.g. Fjell et al., 2009; Good et al., 2001a; Malykhin et al., 2007). Manual volumetric techniques were for a long time considered to be the most reliable method (Jack et al., 1989). There are several variants of manual techniques. For example stereological point counting techniques can be used (Howard et al., 2003). The most traditional variant of manual methods is, however, to simply draw a line around the region that is measured on contiguous slices on a 3D volume acquired by the MRI-scanner.

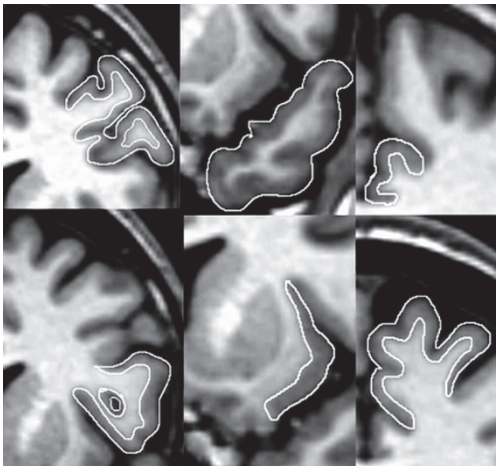

Figure 2
Manual delineation technique of regions in the frontal and temporal lobes (delineation: Olof Lindberg).

Today, there are various automatic techniques available, which can provide several different volumetric parameters, such as cortical thickness, the volume of cortical regions or regional grey matter density in the brain (e.g. Dale et al., 1999; Fischl et al., 1999; Good et al., 2001a).

An interesting perspective on the ongoing improvement of automated volumetric methods is the possibility to measure ever smaller brain regions with maintained precision. Recently an automatic method for measuring hippocampal subfields was developed (Van Leemput et al., 2009). A limitation is, however, that these new methods have to be matched with high quality images from modern MRI scanners to produce reliable results.

2.3 BRAIN REGIONS DISCUSSED IN THE THESIS

For the purpose of illustration, snapshots taken from the Brain-Voyager Tutor (BVT, www.brainvoyager.com) will be used. Regions with no color (grey regions) are not discussed in the illustration.

3 THE FRONTAL LOBE

The human frontal lobe has been described in numerous different ways, depending on the methodology and the criteria of definition (Fuster, 2008). There are three main divisions of the frontal lobe: the prefrontal cortex, the premotor area and the motor cortex.

The motor cortex receives and integrates input from cortical motor and sensory areas and the midbrain, and it has direct projections to the motor neurons of the spinal cord. The area could be described as the "final cortical processing site for voluntary motor commands (Stinear et al., 2009)."

The premotor cortex (PMC) can be divided into one caudal and one rostral sector. The caudal sector has been associated with primary control of actual movements, while the rostral sector is involved in cognitive processing, such as sequence generation, and premotor functions (Abe et al., 2007).

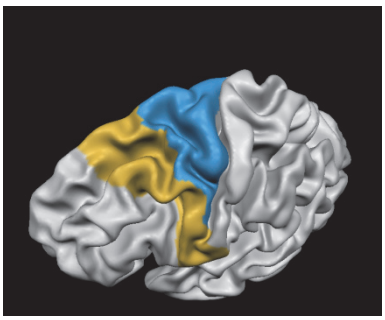

Figure 3
The motor cortex in blue, premotor cortex in yellow, and prefrontal cortex in grey in front of the premotor cortex (image created in BVT).

The prefrontal cortex (PFC) has been described as "the highest level of cortical hierarchy, dedicated to representation of execution and actions (Fuster, 2001)." The PFC has also been described as the highest level in a "synaptic hierarchy" within the frontal lobe (Mesulam, 1998), which encompasses the primary motor area (lowest level), unimodal areas (intermediate level) and heteromodal areas (highest level).

From an evolutionary perspective the PFC has been described as an extension of the motor cortex (Fuster, 2008; Wood and Grafman, 2003). Premotor areas store "motor programs" that are representations of a sequence of more or less complicated movements. During the evolution of the human brain these areas may have evolved to be able to generate efficient strategies for goal-oriented behavior (Wood and Grafman, 2003).

Cognitive theories often emphasize the role of PFC in high order top-down regulation of cognition and behavior (Petrides, 2005). Terms like "supervisory system" and "central executive" have been used to describe these aspects of cognition (Stuss and Alexander, 2007). Güntürkün proposes the following definition of executive functions:

> The PFC is firmly associated with the generation of executive functions, a cluster of cognitive functions that describe the ability to spontaneously generate efficient strategies when relying on self-directed task-specific planning (Güntürkün, 2011).

Thus the frontal lobe and the PFC can be divided in accordance with both structural and functional characteristics. However, multiple definitions are possible for both the structural and functional manner of division.

3.1 STRUCTURAL SUBDIVISIONS OF THE FRONTAL LOBE

The frontal lobe may be subdivided on the basis of the cyto-architectonic characteristics of the cellular structure (Brodmann, 1909; Dombrowski et al., 2001; Petrides et al., 2011), on the basis of regional connectivity to thalamus (Fuster, 2008; Goldman, 1979; Scheibel and Scheibel, 1967) and the on basis of vascular distribution – namely, that different regions of the frontal lobe are supplied by different arteries (Stuss and Benson, 1984) .

Other structural subdivisions are more relevant for this study and these are discussed below.

3.1.1 The cellular structure of grey and white matter

The cortical grey matter on the surface of the brain contains neural cell bodies, neuropil[1], glial cells, astroglia and oligodendrocytes and capillaries. White matter, in contrast, does not contain cell bodies. Instead it contains mostly myelinated axon tracts (Dale et al., 2008).

3.1.2 A division based on the number of cortical layers

In the frontal lobe the posterior orbitofrontal and the anterior cingulate areas are either agranular or dysgranular regions with fewer than six cortical layers, while lateral PFC, M and PMC are an eulaminate cortex with six layers (Barbas and Zikopoulos, 2007; Dombrowski et al., 2001). The laminar pattern is not a random phenomenon. The cellular and laminar structure have been shown to influence the response properties of the neurons in the cortex (Luppino et al., 1991), which at a higher level influence the functional properties of cortical regions (Amunts et al., 2007; Barbas and Zikopoulos, 2007).

3.1.3 Subdivision by gross-anatomy

In gross anatomical terms the cerebral cortex and the frontal lobe may be divided into different gyri and sulci (Crespo-Facorro et al., 2000; Ono et al., 1990; Raz et al., 2004).

[1] A fibrous network of delicate unmyelinated nerve fibers interrupted by numerous synapses and found in concentrations of nervous tissue especially in parts of the brain where it is highly developed.

Gyri and sulci have traditionally been used as indirect landmarks for cyto-architecture. For higher, multimodal, cortical areas, however, such landmarks may be highly unreliable (Amunts et al., 2007; Fischl et al., 2008). Unimodal primary or secondary cortices may, on the other hand, be well predicted from the location of sulci and gyri (Fischl et al., 2008; Welker and Seidenstein, 1959) (See further in section 3.2.2.).

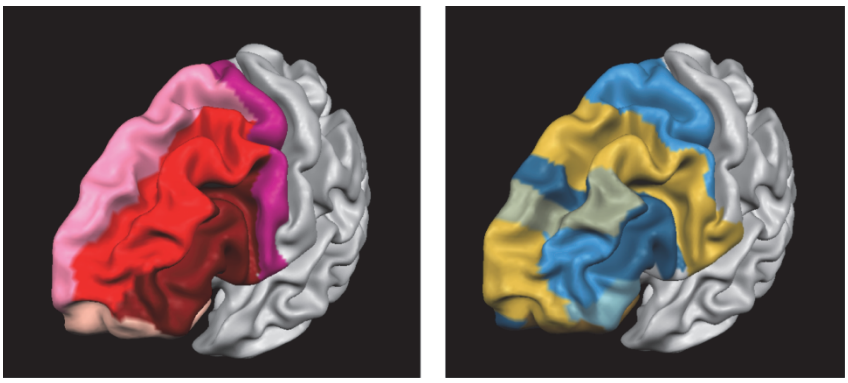

Figure 4
The relationship between cytoarchitecture and gross-morphology in the frontal lobe.
To the left the gross morphological appearance of the superior, middle, inferior and precentral gyrus. Pink: superior frontal gyrus, Red: middle frontal gyrus, Brown: inferior frontal gyrus. Darker pink color: precentral gyrus. To the right: The frontal lobe is shown divided into different cyto-architectonic (Brodmann) areas. The colors represent different Brodmann areas. Image created in BVT.

3.1.4 Division based on the regional connectivity

Conceptually the whole brain could be viewed as a large-scale network operating at several levels of information processing ranging from groups of neurons, to local circuits, to systems of brain areas (Errington et al., 2003). Different cortical systems are also commonly associated with different cognitive or emotional aspects of human behavior.

The frontal lobe may be divided into systems on basis of its regional connectivity. Cortical areas within one system or network are preferentially interconnected with other regions within the same system (Price and Drevets, 2010), however each system also has a characteristic pattern of connectivity with regions outside the system. According to this viewpoint the frontal lobe may be divided into the orbitofrontal, medial, dorsal, ventral and caudal networks (figure 5).

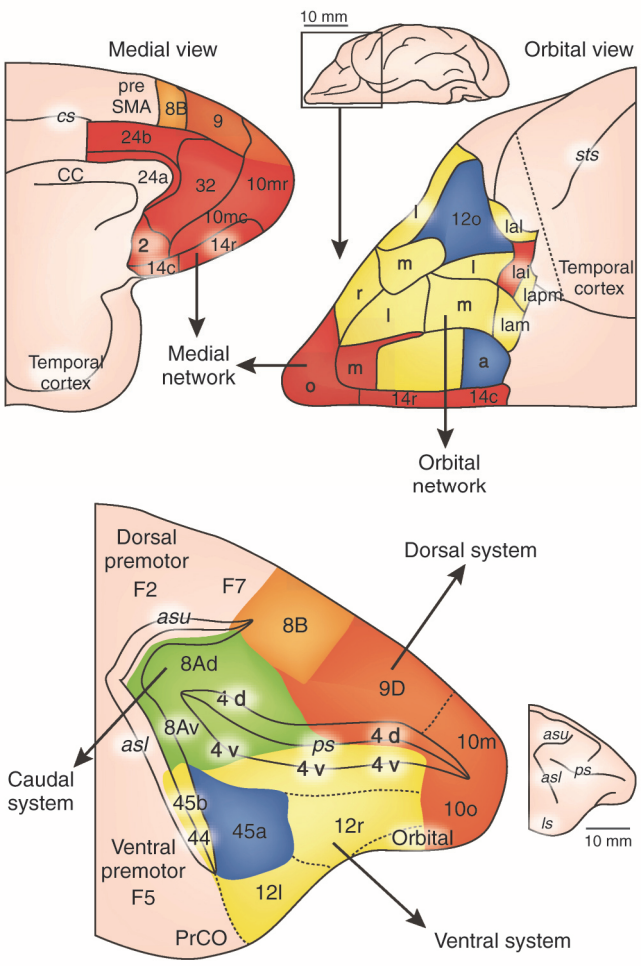

Figure 5
Division of the frontal lobe based on regional connectivity. The three regions displayed in blue belong to more than one network. There is a gradual change in the pattern of connectivity in the dorsal system, which is illustrated by the changing color nuance between area 9D and 8B.
The white-colored spots are sites in which retrograde and antrograde tracers were injected in studies on monkey. *Reprinted by permission from Macmillan Publishers Ltd: Neuropsychopharmacology (Neurocircuitry of Mood Disorders, Price & Drevets, Neuropsychopharmacology 35, 192–216), copyright (2010).*

The *orbitofrontal network* has connections with all sensory systems (Barbas, 2000), and the system has been suggested to integrate multi-modal stimuli. As will be discussed below this network seems to be important for assessing the value of stimuli (Price and Drevets, 2010) and reward guided behavior (Buckley et al., 2009).

The *medial network*, located on the ventromedial surface of the frontal lobe, has strong limbic connections. Both amygdala and hippocampus project directly to this region (Barbas and Blatt, 1995; Ongur and Price, 2000). It also has a characteristic output into visceral control areas in the hypothalamus and to the periaqueductal grey (Price and Drevets, 2010). In contrast to the orbital system that to a large extent can be viewed as a sensory input system, the medial system has the ability to modulate visceral functions

in response to emotions and other factors (Price and Drevets, 2010). The medial network has connections to the superior temporal sulcus and gyrus, the entorhinal cortex, the parahippocampal gyrus as well as the anterior and posterior part of the cingulate gyrus (Saleem et al., 2008).

The *dorsal network* has close connections with the medial network and shares many of its connections. Both networks are connected to the superior temporal gyrus, anterior and posterior cingulate cortex, the entorhinal cortex as well as the parahippocampal gyrus, and both networks project to the hypothalamus and to the periaqueductal grey (Price and Drevets, 2010).

The *ventral network* is closely interacting with and has many connections in common with the orbitofrontal network. It seems, however, that the ventral network lacks olfactory and taste input. It has been proposed that the ventral network takes part in the assessment of non-food sensory objects (Price and Drevets, 2010). It is connected with visual areas in the inferior temporal cortex and to dysgranular regions in the insula and frontal operculum that are related to somatic-sensory functions (Price and Drevets, 2010).

The *caudal network* in the lateral prefrontal cortex has sometimes been described as part of the dorsal attention system (Corbetta et al., 2002; Vincent et al., 2008). It includes the frontal eye field and has connections with the dorsal premotor cortex, posterior superior temporal sulcus and posterior parietal cortex. One specific function of this network is to control saccadic eye movement (Price and Drevets, 2010).

Apart from the systems described above there is also one prefrontal region, Brodmann Area 45a (denoted in blue in figure 5), that seems to be connected to all parts of the lateral prefrontal cortex. This region has many connections in common with the medial and dorsal network but it also has connections to more posterior parts of the superior temporal gyrus including some auditory regions. It is suggested that this region may be a multi-modal cortex that has connections with emotional circuits of the brain (Price and Drevets, 2010).

3.2 FUNCTIONAL SUBDIVISIONS OF THE FRONTAL LOBE

3.2.1 Divisions based on cognitive or emotional functions

It is a long established knowledge that different parts of the brain are involved in, or essential for different emotional, cognitive or behavioral processes. Already 1700 B.C. the “Edwin Smith Papyrus” was written. This papyrus seems to be a surgical textbook which discusses the relationship between injuries in the brain and spinal cord and their consequences for bodily functions (Coles et al., 2008).

Modern research on the functional specificity of cortical regions may however have started with two famous patients with localized lesions in the frontal cortex.
In 1861 Paul Broca treated a patient with a lesion in the frontal lobe. This patient lost the ability to produce fluent speech, and was after the lesion only able to say the

nonsense word “Tan” (Broca, 1861). The patient died shortly afterwards and was at post mortem exam found to have a lesion in the left inferior frontal gyrus. Broca thus hypothesized that this region was fundamental for production of spoken language. This case also started the research on functional hemispheric lateralization in the brain (Teive et al., 2011).

The second famous case is the story of Phineas Gage (Ratiu and Talos, 2004). He had a severe lesion in the brain, caused by a traumatic accident in which an iron rod was driven completely through his left frontal lobe. The original report on this case was written in 1848, however it has been reprinted as a “classical case report” (Harlow, 1999). Unexpectedly Gage survived this accident and was first thought to have been fully recovered. However:

> Previous to his injury, although untrained in the schools, he possessed a well-balanced mind, and was looked upon by those who knew him as a shrewd, smart businessman, very energetic and persistent in executing all his plans of operation. In this regard his mind was radically changed, so decidedly that his friends and acquaintances said he was “no longer Gage” (http://www.deakin.edu.au/hmnbs/psychology/gagepage/).

Thus, following a lesion to the anterior frontal lobe, Gage’s behavior had changed so drastically that his friends found him to be another person.

Interestingly these two famous cases do, to a large extent, display the same symptoms as two variants of FTLD. Patients with progressive nonfluent aphasia (PNFA) have very similar symptoms as Broca’s patient, while some patients with frontotemporal dementia (FTD) have symptoms similar to those displayed by Phineas Gage. The localization of brain damage in these two variants of dementia is also very similar to these two famous cases (this will be discussed in detail below).

The research on brain lesions has continued in recent years both on humans and in monkeys. In one study macaque monkeys were trained to perform a Wisconsin Card Sorting test analog (for a description of the test see Gormezano and Grant, 1958). After training lesions were induced in specific prefrontal brain areas of the animals. Results suggest that different frontal lobe regions contribute to different cognitive “components” of this test (Buckley et al., 2009): Lesions of the *principal sulcus* (mainly corresponding to the middle frontal gyrus in humans) impaired maintenance of abstract rules in working memory. Lesions of the *orbitofrontal cortex* impaired a rapid reward-based updating of representation of rules value - in this case whether a certain strategy of sorting cards were related to a reward or not. Lesions of the *anterior cingulate gyrus* impaired active reference to the value of recent choice-outcomes during rule-based decision making. Lesions of the *ventrolateral prefrontal cortex* impaired the ability to learn and implement new rules.

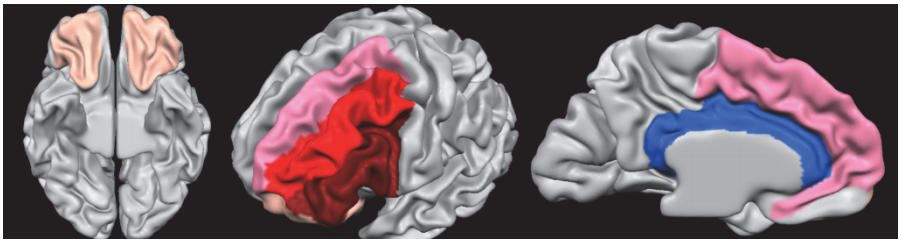

Figure 6
The approximate location of the regions discussed by Buckley et al. The orbitofrontal cortex is shown to the left in pale pink, the dorsolateral and ventrolateral are shown in middle (the dorsolateral region encompasses the lateral part of the superior frontal gyrus in pink and the whole middle frontal gyrus in red). The ventrolateral region is displayed in brown in the middle image. To the right anterior cingulate gyrus which is the anterior part of the blue region (the pink color in image to the right is the middle surface of the superior frontal gyrus). Illustration created in BVT.

In several different studies Donald Stuss and colleagues have investigated the effect of frontal lobe lesions in humans (Stuss and Alexander, 2007). In a "revamped attention model" (Stuss, 2011) they propose that three different cognitive components may be related to three different parts of the frontal lobe:

- *Energization*: The process to initiate and sustain a response. This ability is impaired in patients with *superior medial prefrontal* (Brodmann area (BA) 24, 9 and 6) lesions.
- *Task setting*: The ability to set a stimulus-response relationship. This ability is impaired particularly in patients with *left lateral* (BA 44, 45, 46, 9 9/46 and 47/12) lesions.
- *Monitoring*: The process of checking the task over time for 'quality control' and the adjustment of behavior. This ability is impaired in patients with *right lateral* (BA 44, 45, 46, 9 9/46 and 47/12) lesions.

It is further suggested that two other cognitive domains may be disturbed by frontal lesions (Stuss, 2011):

- *Social behavior*: Dysfunction in the ability to integrate motivational (reward-based), emotional, and social aspects of behavior may be impaired in patients with lesions of the *ventromedial prefrontal cortex* (BA 32, 25, 24, 13, 12 and 11).
- *Metacognition/integration*: The ability to orchestrate the energization, motivation, emotional and executive aspects of a complex task [called "hyper-monitoring" by Petrides (2005)] is impaired in patients with lesions in the frontopolar region (BA 10s and 10i).

3.2.2 Division based on synaptic hierarchies

Another functional subdivision of the frontal lobe is based on the complexity of the task that is performed in a specific area. This can be described by a "synaptic hierarchy" (Mesulam, 1998), in which the brain can be divided into primary sensory, unimodal, heteromodal, limbic and paralimbic zones. Interestingly the neurodevelopmental pattern from young to old age may differ at different levels of the synaptic hierarchy. Thus heteromodal areas have been shown to have a more complex volumetric trajectory during development (Shaw et al., 2008), and a longer maturation process than primary sensory, unimodal and limbic regions (Casey et al., 2005; Gogtay et al., 2004; Westlye et al., 2010b). The heteromodal areas of the brain have also been shown to be more vulnerable to age-related changes at old age, while primary areas and unimodal areas have been found to be more vulnerable at very old age (above the age of 80) (McGinnis et al., 2011).

4 VOLUMETRIC STUDIES OF THE BRAIN

4.1 VOLUMETRIC STUDIES IN HEALTHY AGING

Volumetric studies on structural MRIs is a well-established method to study effects of pathology (Lindberg et al., 2009; Whitwell and Jack, 2005) and aging in the brain (McGinnis et al., 2011; Raz et al., 2005; Tisserand et al., 2002; Walhovd et al., 2011).

A common approach is to investigate regional grey matter volumes or the regional thickness of the cortex. Volumetric studies on the cortex suggest that cortical thinning occurs during healthy maturation at young age, which has been related to synaptic pruning in the mid-to-late adolescence (Sowell et al., 2001; Toga et al., 2006). Cortical thinning is also occurring during aging, which according to a recent review only to a minor extent is caused by the loss of neurons. Instead volume loss seems to be caused by the shrinkage of neurons, reduction of synaptic spines and the lowering of the number of synapses (Fjell and Walhovd, 2010).

Another approach is to measure the volume of combined grey and white matter of cortical regions. This has for example been done by measuring the total volume of the gyri of the frontal lobe in aging (Convit et al., 2001) or in neurodegenerative diseases (Perry et al., 2006). A methodological consideration in such an approach is that age- or pathology related shrinkage may progress at different rates in grey and white matter. In a large study (including 883 subjects) the rate of cerebral white and grey matter shrinkage was investigated (Walhovd et al., 2011). This study found the highest rate of shrinkage in cortical grey matter at 40-59 years of age (-7,9%) while the highest rate in white matter was found at 70-95 years of age (-8,5%).

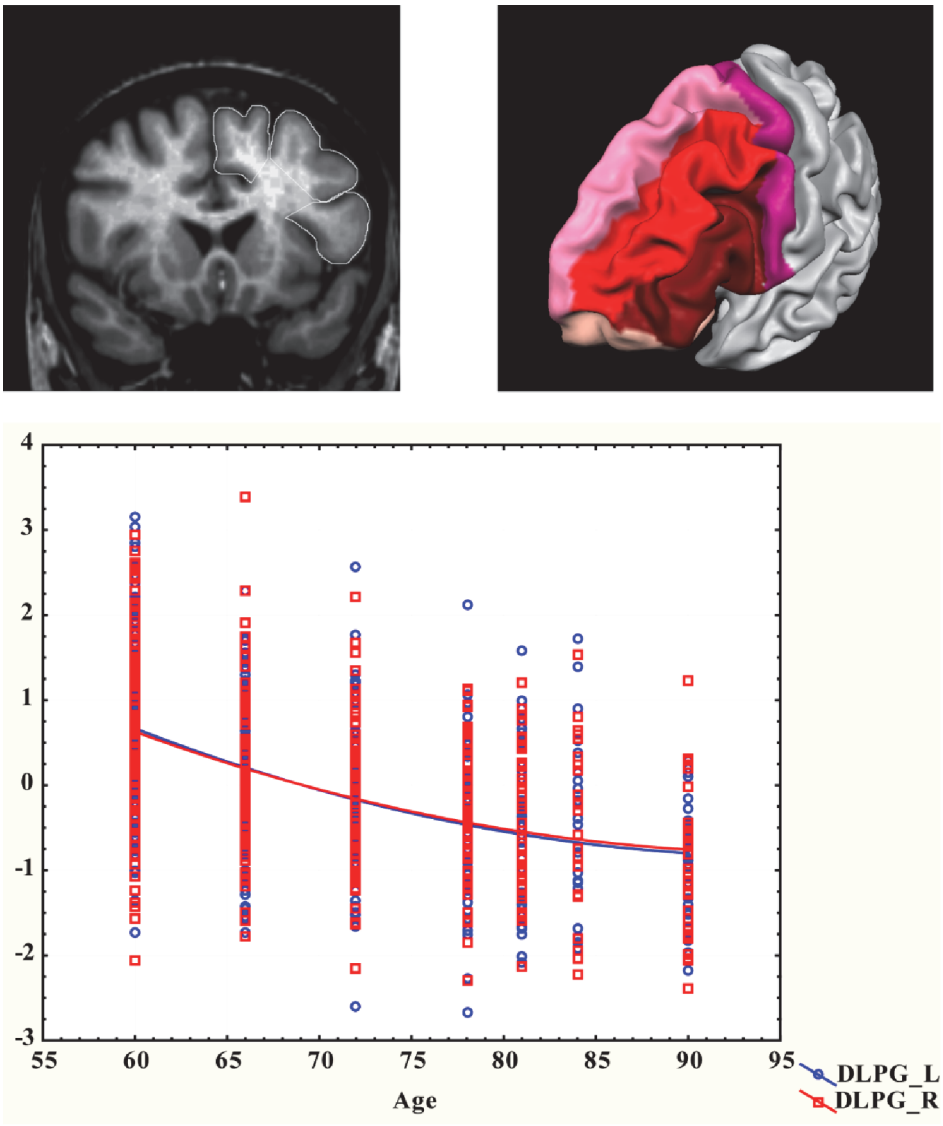

Figure 7
Volumetric results of manual delineation of the superior, middle and inferior frontal gyrus in 505 normal aging adults 60-97 years of age. The population is described further in study IV. Above left: An example of delineation of the frontal gyri. Above right: The region measured illustrated by BVT (region in pink: superior frontal gyrus, in red: middle frontal gyrus, in brown: inferior frontal gyrus). The bottom graph illustrates volume loss in the left and right side of the superior and middle frontal gyrus which have been combined into one region, the dorsolateral prefrontal gyri (DLPG_L: on the left side, DLPG_R: on the right side). The X-axis denotes age, and the Y-axis displays the volume of the gyri divided by the intra-cranial volume normalized as z-scores. Volumetric data obtained by Olof Lindberg (unpublished results).

In last chapter, different methods for dividing the frontal lobe were reviewed. Interestingly the structural characteristics of the brain may be important for predicting how volume loss occurs both in maturation and aging. Below some hypothesis on the relationship between brain structure and age-related volume loss are presented.

4.1.1 Age-related volume loss and cortical structure

Several studies have found pronounced age-related volume loss in the prefrontal cortex (for a review, see McGinnis et al., 2011). This region and other heteromodal areas have also been shown to display a longer maturation process than most other parts of the brain (Casey et al., 2005; Gogtay et al., 2004; Westlye et al., 2010b). This has led to the so-called "*last in*, (last to mature) *first out* (first to show age-related volume loss) *hypothesis*" (McGinnis et al., 2011). Recent findings, however, suggest that the last in-first out hypothesis is valid mostly in adults between 30-60 years of age. At very old age (above 80 years) primary sensory and unimodal areas may display the largest cortical volume loss (McGinnis et al., 2011).

Another hypothesis suggests that age-related shrinkage starts in the anterior parts of the brain and successively moves posteriorly (Walhovd et al., 2011). This phenomenon has been demonstrated along the white matter tracts (Davis et al., 2009) and in grey matter (Raz et al., 2004). In a recent review however, it is suggested that such gradient in grey matter may be more related to vascular diseases than to aging (Raz and Rodrigue, 2006; Raz et al., 2007).

Some findings suggest that the cortical and subcortical structures of the limbic system may be better preserved in aging than other brain regions (Grieve et al., 2005). One hypothetical explanation for this is that limbic and paralimbic structures, like the hippocampus, are of fundamental importance for sensory integration, arousal and memory. It would thus from an evolutionary point of view be necessary for these regions to be preserved for humans to survive and function also in their old age (Grieve et al., 2005). A recent study, however, suggests that volumetric change in the maturation process, at young age, and volume loss, at old age, may differentially affect different limbic regions (Grieve et al., 2011).

4.2 VOLUMETRIC STUDIES AND COGNITION IN HEALTHY AGING

In aging adults larger cortical grey matter volume is sometimes associated with better performance on cognitive tests. One study found for example a positive correlation between the grey matter volume of the gyrus rectus (on the orbital surface of the frontal lobe) and scores on sequencing and nonverbal abstract reasoning tests in healthy elderly subjects (Elderkin-Thompson et al., 2009).

In section (4.1) it was shown that a common finding is the association between loss of regional brain volume and aging, particularly in the frontal lobe (Tisserand et al., 2002; Walhovd et al., 2011). Thus larger cortical volumes in aging may be associated with a

better preservation of the brain, which at the next level may be linked to better performance in cognitive tests.

Old adults may however differ significantly with respect to the amount of brain volume lost (Raz et al., 2010). This often causes a larger variance in regional brain volumes between old adults at the same age than in young adults, at the same age. The variance in volumetric data may also be related to a larger variance in cognitive performance. One study found for example a stronger association between the cortical thickness of the dorsolateral prefrontal cortex and the performance on the Wisconsin Card Sorting Test in older adults (60-71 years of age) than younger adults (20-32 years of age) (Burzynska et al., 2011). As suggested in a recent review cortical thinning is among other things related to a reduction of synaptic spines and lower number of synapses (Fjell and Walhovd, 2010). This may reduce the connectivity between different brain regions, which at the next level may result in poorer performance on cognitive tests.

4.3 VOLUMETRIC STUDIES IN PAHTOLOGICAL AGING

Cortical and subcortical volume loss generally occurs at much higher rate in neurodegenerative diseases (McEvoy et al., 2011). Different brain networks are affected in different neurodegenerative diseases (Tartaglia et al., 2011), which is manifested in volume loss in regions belonging to those networks, and furthermore in the clinical symptoms displayed by the patient.

4.3.1 Genetics, pathology and clinical symptoms

A fundamental question in any volumetric study on dementia patients is the procedure for classifying or diagnosing the illness of these patients. This is a complicated issue since several different classification methods are possible. Patients may be classified on the basis of genetics, on the basis of pathology, on the basis of pattern of brain atrophy or on the basis of clinical symptoms. A particular problem is that different classification procedures may come to different conclusions regarding diagnosis. One study, for example, found that 44% of patients that fulfilled the clinical criteria for PNFA (a FTLD variant) was at post mortem found to display the neuropathological hallmarks of AD (Alladi et al., 2007).

Tartaglia et al. have summarized the aims and scope of a volumetric study on clinically diagnosed dementia patients:

> Volumetric studies aimed at gaining an understanding of brain-behavior relationships have demonstrated relationships between focal changes in brain volume and cognitive or behavioral changes in dementia (Tartaglia et al., 2011).

In this sense a volumetric study on clinically diagnosed patients has many factors in common with the studies on patients with brain lesions discussed in section (3.2) (Stuss and Alexander, 2007; Stuss, 2011). In both approaches the main focus is to establish a relationship between brain damage and cognitive or behavioral symptoms. However, similar clinical symptoms may be caused by different variants of brain pathology

(Alladi et al., 2007). It should furthermore be noted that clinical symptoms, which potentially could be caused by atrophy of certain brain regions, might also be present without atrophy of these regions. In a visual rating study of 51 FTD, 22 PNFA and 52 semantic dementia (SD) patients it was found that 47% of the FTD and 29% of the PNFA patients did not display any abnormalities in the MRI scans (Kipps et al., 2007). Interestingly, however, 100% of the SD patients had abnormal scans.

In this thesis all dementia patients were diagnosed in accordance with consensus criteria for clinical symptoms: for FTLD in accordance with criteria proposed by (Neary et al., 1998), for AD in accordance with DSM IV-R (Diagnostic statistical manual of mental disorders revised version) (American Psychiatric Association, 2000) and International Classification of Diseases tenth revision (ICD-10; WHO, 1992).

4.3.2 Consensus criteria for FTLD

In the following section the characteristic symptoms in the FTLD subtypes and in AD are discussed. Clinical terms are defined in the appendix (section 9).

The clinical international consensus criteria for FTLD include three syndromes: frontotemporal dementia (FTD), progressive nonfluent aphasia (PNFA), and semantic dementia (SD) (Neary et al., 1998). FTD is diagnosed primarily on the basis of early decline in interpersonal conduct, early emotional blunting, and an early loss of insight or concern about such changes. This transformation of character should be the dominant feature at onset and throughout the disease.

The diagnosis of PNFA is made in patients who insidiously develop nonfluent speech with agrammatism (a pattern of simplified sentence structure), phonological paraphasias, or anomia. Apraxia of speech is a common feature whereas word comprehension and comportment are preserved initially.

SD, in contrast, is defined by fluent but “empty” spontaneous speech, anomia combined with impaired word comprehension and associative agnosia or prosopagnosia. Surface alexia and surface agraphia may occur in patients who use alphabetic scripts.

4.3.3 Consensus criteria for AD

For the diagnosis of AD the *Diagnostic and statistical manual of mental disorders* (4th ed.) requires memory deficits as a core diagnostic feature, in addition to at least one of the following symptoms: aphasia, apraxia, agnosia or deficits in executive functioning (American Psychiatric Association, 2000).

4.4 CLINICAL SYMPTOMS AND BRAIN ATROPHY IN FTLD AND AD

4.4.1 AD

The core clinical symptom of AD is memory deficits. The "system" involved in memory processing has sometimes been described as the hippocampal-cortical-memory system. This network is active during passive mental states that have been associated with internally directed cognition, such as memories of past events and thinking about the future (Vincent et al., 2008).

Using resting state functional MRI Vincent et al found that activity in the hippocampal formation correlated with several other regions including the ventromedial prefrontal cortex, dorsal frontal cortex, lateral temporal cortex, posterior cingulate cortex and ventral posterior inferior parietal lobule. This system, they suggest, is the hippocampal-cortical-memory system (Vincent et al., 2008).

At a neurophysiologic level retention of explicit (conscious) memories can be described as a process involving different types of cortical regions. Initial processing occurs in one or more polymodal association cortices (prefrontal, limbic or parietal-occipital-temporal cortices), which synthesize visual, auditory and somatic information. From polymodal areas the information is sent further to parahippocampal and perirhinal cortices and then to the entorhinal cortex, the dentate gyrus, the hippocampus and the subiculum. Information is then sent back to the polymodal areas in the opposite direction: From the subiculum to the entorhinal cortex, the parahippocampal and the perirhinal cortex to the polymodal areas (Kandel et al., 2000).

The structures of the medial temporal lobe are thus of fundamental importance for the consolidation of memories. Kandel proposes that the hippocampus and the rest of the medial temporal lobe may act over a long period of time (even weeks) to facilitate storage of information. He presents the following example: Cells in the visual association cortex in the inferotemporal lobe initially process storage of the information about a face. These cells are interconnected with other areas that support additional knowledge about the person whose face is seen. These connections can be modulated by the hippocampus (Kandel et al., 2000), through a mechanism called long-time potentiation (Bliss and Collingridge, 1993).

In studies on post mortem brains it has been shown that the entorhinal cortex as well as regions of the limbic systems are affected relatively early on by pathology in AD (Braak et al., 1996). Thus the key structures for memory consolidation are the regions that are affected in AD.

4.4.2 FTLD

4.4.2.1 Frontotemporal dementia

In patients with FTD a core symptom may be alteration of personality and social behavior. Such personality changes are usually related to atrophy of the orbitofrontal cortex and ventromedial prefrontal cortex (Rabinovici and Miller, 2010). In some patients apathy is the most pronounced symptom (Rabinovici and Miller, 2010; Rosen et al., 2005), which is related to atrophy in the dorsomedial frontal lobe (Rabinovici and Miller, 2010).

The relationship between dorsomedial atrophy and apathy could be interpreted as consistent evidence for the theory about "energization" proposed by Stuss and colleagues discussed in section 3.2.1 (Stuss and Alexander, 2007; Stuss, 2011).

The relationship between orbitofrontal atrophy and personality changes may potentially be explained by the so-called "somatic-marker" hypothesis (Viskontas et al., 2007) proposed by Damasio (Damasio, 1996). In section (3.1.4) the orbital network is discussed. This network receives input from all sensory modalities (Barbas, 2000; Price and Drevets, 2010). Damasio speculates that this network is of fundamental importance for linking a stimulus to an evaluative bodily signal (Damasio, 1996), which may be thought of as an autonomic state that is induced by the circumstances of the situation (Viskontas et al., 2007). In light of the review of the main network of the frontal lobe, it may be suggested that the "resultant autonomic state" is potentially not a function of the orbital network but rather of the adjacent medial prefrontal network (Price and Drevets, 2010).

In recent years, however, several studies have found a number of weaknesses in the somatic-marker hypothesis (Bennett and Hacker, 2005). It has been pointed out that Damasio reduces the essence of a feeling or an emotion to the experience of a bodily state. It has also been suggested that some feelings like gratitude may not involve any somatic disturbance at all (Bennett et al., 2005).

Nevertheless, while some aspects of the emotional processing system may not be fully understood, it has been repeatedly shown that atrophy of the orbitofrontal and the ventromedial prefrontal cortex has been associated with alteration of social and emotional behavior in FTD (Rosen et al., 2005; Viskontas et al., 2007).

4.4.2.2 Progressive nonfluent aphasia

The core symptom in PNFA is that patients insidiously develop nonfluent speech. This has been related to atrophy of cortical areas responsible for speech production. The neurophysiologic process underlying speech production is, however, complicated and involves several different steps. Activation of speech sound "map cells" (Guenther, 2006) occurs first. These cells are hypothesized to be located in the posterior part of Broca's area, in a region sometimes referred to as the frontal operculum. It has been suggested that the sound map cells "read out motor plans" for chunks of well-learned speech sounds (Bohland and Guenther, 2006), and it has been shown in fMRI that the activation of the frontal operculum increase when a complex sentence requires multiple speech sounds (which thus is hypothesized to be related to the activation of multiple

sound map cells). The activation of speech sound maps is followed by motor commands that reach the motor cortex via a control system that can be divided into two subsystems: a feedforward control system and a somatosensory and auditory feedback control system (Guenther, 2006).

An alternative way of describing the function of the frontal operculum is that it is a higher level area that predicts the auditory and motor consequences of speech (Price et al., 2011).

Another region that has been shown to be important in speech production is the left anterior insula. However, contrary to the inferior frontal gyrus, this region may be involved in the coordination of complex articulation (Baldo et al., 2011).

Thus several different levels of speech processing could potentially be involved in the clinical symptoms of PNFA. Neuroimaging studies of this syndrome have, however, revealed that the earliest site of atrophy is commonly found in the inferior frontal gyrus and the anterior insula (Gorno-Tempini et al., 2004).

4.4.2.3 Semantic dementia

A key symptom in SD is the peculiar loss of factual knowledge and word meaning (Neary et al., 1998). This has been related to pathology of the anterior temporal lobe, which often, but not always, is more predominant on the left side (Seeley et al., 2005).

Several theories have been proposed about the functionality of the anterior temporal lobe for retention and recall of semantic knowledge. Earlier studies suggest that this region may serve as a "hub" connecting sensory-specific and semantic associations (McClelland and Rogers, 2003; Patterson et al., 2007). The symptoms of SD could be interpreted as support for this hypothesis (Seeley et al., 2005).

A recent finding, however, suggests that a "semantic hub" may be located posterior to the temporal pole, possibly in the left anterior fusiform gyrus (Skipper et al., 2011). Evidence for this hypothesis was found in one fMRI study in which participants performed semantic memory tasks. Peak activations were found in the anterior-medial fusiform gyrus (Binney et al., 2010).

In light of these new findings the interpretation of the relationship between atrophy and clinical symptoms in SD could potentially be reevaluated. Previous studies suggest that while atrophy may start on side of the anterior temporal lobe it will later progress to the same region on the contralateral side (Seeley et al., 2005). A recent study found that lesions in either the left or right anterior temporal pole did usually not produce the symptoms of SD, which suggests that bilateral temporal lobe damage is normally required to generate a clinically notable disruption to conceptual knowledge (Lambon Ralph et al., 2010).

I suggest that another way of interpreting this may be that *if* atrophy has progressed to the contralateral temporal pole, it may also have spread posteriorly in the ipsilateral hemisphere, thus involving the anterior fusiform gyrus (the potential location of the "semantic hub").

Evidence that the progression of atrophy in SD may occur in this manner has been presented in a previous study (Seeley et al., 2005), as well as in results presented by us.

In study I of this thesis we investigated 13 SD patients. A separate analysis revealed that 4 of these patients had more atrophy in the right than left temporal lobe, while 9 had more atrophy in the left than right temporal lobe. If the SD group is divided into SDL (SD patients with predominantly left side atrophy) and SDR (SD patients with predominantly right side atrophy), statistical analysis reveals that there is no significant difference between SDL and SDR in volume of the right temporal pole. However there is a significant difference between groups in the volume of the right anterior hippocampus (see figure 8). This might be interpreted as follows. At initial stages the anterior temporal lobe becomes atrophic either on the left or on the right side in SD. As the disease develops the contralateral temporal lobe (that was initially spared) also becomes atrophic. At the same time atrophy progresses more to the posterior in the temporal lobe that first displayed volume loss, which would make the right anterior hippocampus more affected in patients that first had atrophy in the right temporal pole than in patients that first had atrophy in the left temporal pole.
These results could potentially support my interpretation that if atrophy has reached more posteriorly in the left temporal lobe it is also very likely that is has progressed to the right temporal pole. If atrophy develops in this manner it could account for the recent finding, discussed above, that bilateral anterior temporal atrophy is needed to produce the symptom of SD.

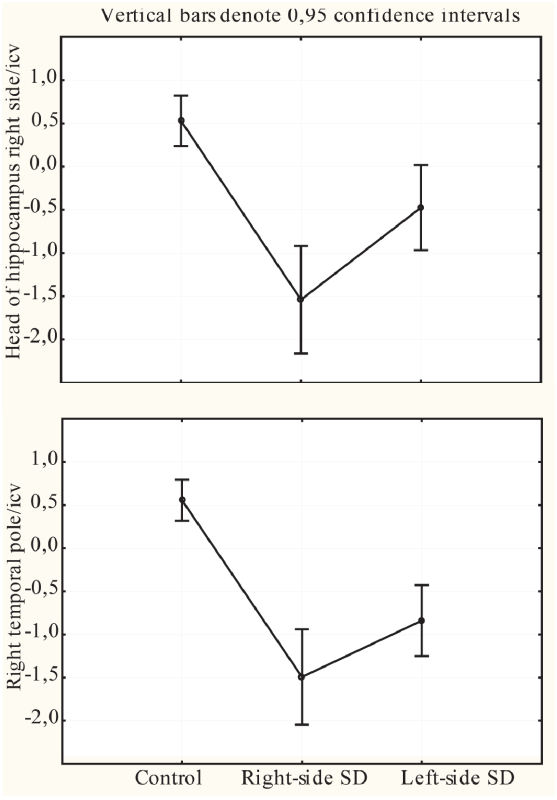

Figure 8

The volume divided by intracranial volume normalized as z-scores of the right temporal pole and the right anterior hippocampus in SD patients with predominantly right side (Right-side SD) and predominantly left side (Left-side SD) atrophy. The volume of the right anterior hippocampus was significantly smaller in right-side SD than in left-side SD, but there was no significant difference between these subgroups in the right temporal pole (data presented at the International School of Neuroanatomy in Sicily, 2011).

Another symptom in SD is deficits in social comprehension (Shany-Ur and Rankin, 2011). This may support recent findings which suggest that the temporal pole is involved in the processing of social knowledge (Skipper et al., 2011).

4.5 CONNECTIVITY AND PROGRESSION OF ATROPHY IN DEMENTIA

Above some central and early sites of atrophy in AD and the subtypes of FTLD are discussed. An interesting finding is that the anatomical connections of the early sites of atrophy may partly determine how atrophy progresses in dementia. It is proposed that regions that become affected later in a neurodegenerative disease have anatomical connections with regions that are affected early (De Lacoste and White, 1993; Pearson et al., 1985; Seeley et al., 2009).

The underlying mechanism for this has been suggested to be that molecular pathologies such as β-amyloid, tau, α-synuclein and TDP-43 progress through specific anatomical connections or brain networks (Rönnback et al., 2011; Seeley et al., 2009). In volumetric studies, progression of molecular pathologies in neurodegenerative diseases has been demonstrated by showing that regions that become atrophic later during the course of a neurodegenerative disease bear known anatomical connections with regions that become atrophic early (Seeley et al., 2009). Interestingly, an opposite effect may also cause atrophy between two anatomically connected regions. In early studies on the connectivity of the sensory systems of the brain, Jonas and Powell (1970) have shown that if a lesion is induced in one area within one sensory system, degeneration is produced in the areas that have close anatomical connections with the damaged area. In this case the neurodegeneration is not caused by a progression of pathological molecules but rather by other mechanisms such as the degeneration of axons.

An interesting phenomenon in patients with SD is that they present with severe temporal but limited or no frontal atrophy (Lindberg et al., 2009). A potential method to investigate pathological progression of atrophy could thus be to investigate what parts of the frontal lobe that have the closest connections with the severely atrophic temporal lobes.

The hippocampus, which shows severe atrophy in SD (see study I & III), has unidirectional anatomical projections to the ventromedial and in particularly the subcallosal ventromedial prefrontal cortex (SMPC) (Barbas and Blatt, 1995; Kahn et al., 2008). SMPC belongs to the medial frontal network that is discussed in section 3.1.4 and displayed in figure 5.

Apart from the connections with the temporal lobe and hippocampus the SMPC also has connections with many regions of the frontal cortex (for example areas within the orbitofrontal cortex).

Because of its anatomical connections to both frontal and temporal regions that become pathological early in FTLD it could be hypothesized that the SMPC will become atrophic in all variants of this syndrome. In figure 9 we have investigated the correlation between the total volume (left side + right side) of the SMPC, the total volume of the orbitofrontal cortex and the total volume of the hippocampus in SD and

FTD in patients included in study III (for volumetric protocol of the SMPC see appendix).

The figure reveals that the total volume of the SMPC is correlated with the total volume of the orbitofrontal cortex in FTD, while it is correlated with the total volume of the hippocampus in SD. This could potentially reflect a progression from initial temporal atrophy in SD.

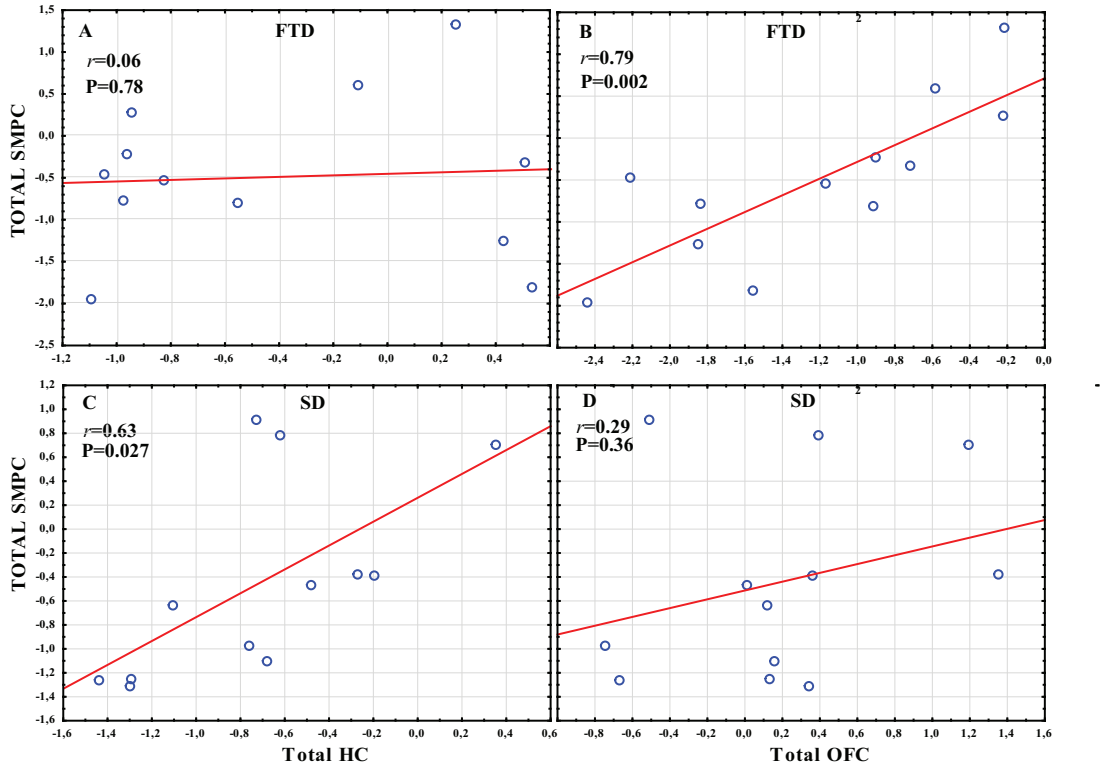

Figure 9
The correlation between the total volume of the subcallosal ventromedial prefrontal cortex, the total volume of the orbitofrontal cortex and the total volume of the hippocampus in SD and FTD (unpublished data. For description of included patients see study III).

Interestingly the strength of the anatomical connections may determine how fast atrophy spreads from one region to another. The SMPC is potentially the frontal region that receives the strongest projections from the anterior temporal lobe, although some parts of the orbitofrontal cortex also receive anterior temporal projections (Ongur and Price, 2000). The dorsolateral prefrontal cortex on the other hand is at multisynaptic distance from the anterior temporal lobe. In figure 10A we see that this is directly reflected in the degree of atrophy of the frontal regions in SD. Thus SMPC displays significant volume loss compared to controls, the orbitofrontal cortex displays some volume loss while the dorsolateral prefrontal cortex has no volume loss. Figure 10B shows measurements of the same regions in AD. As in SD we find volume loss in temporal regions, the SMPC and the OFC. However, the AD patients have on the whole much milder degrees of atrophy than the SD patients. Thus only the temporal regions display significant volume loss compared to controls. The pattern of volume loss is however almost identical to the pattern found in SD, which may indicate that volume loss in the SMPC will become significant as temporal atrophy increases during the progression of the disease.

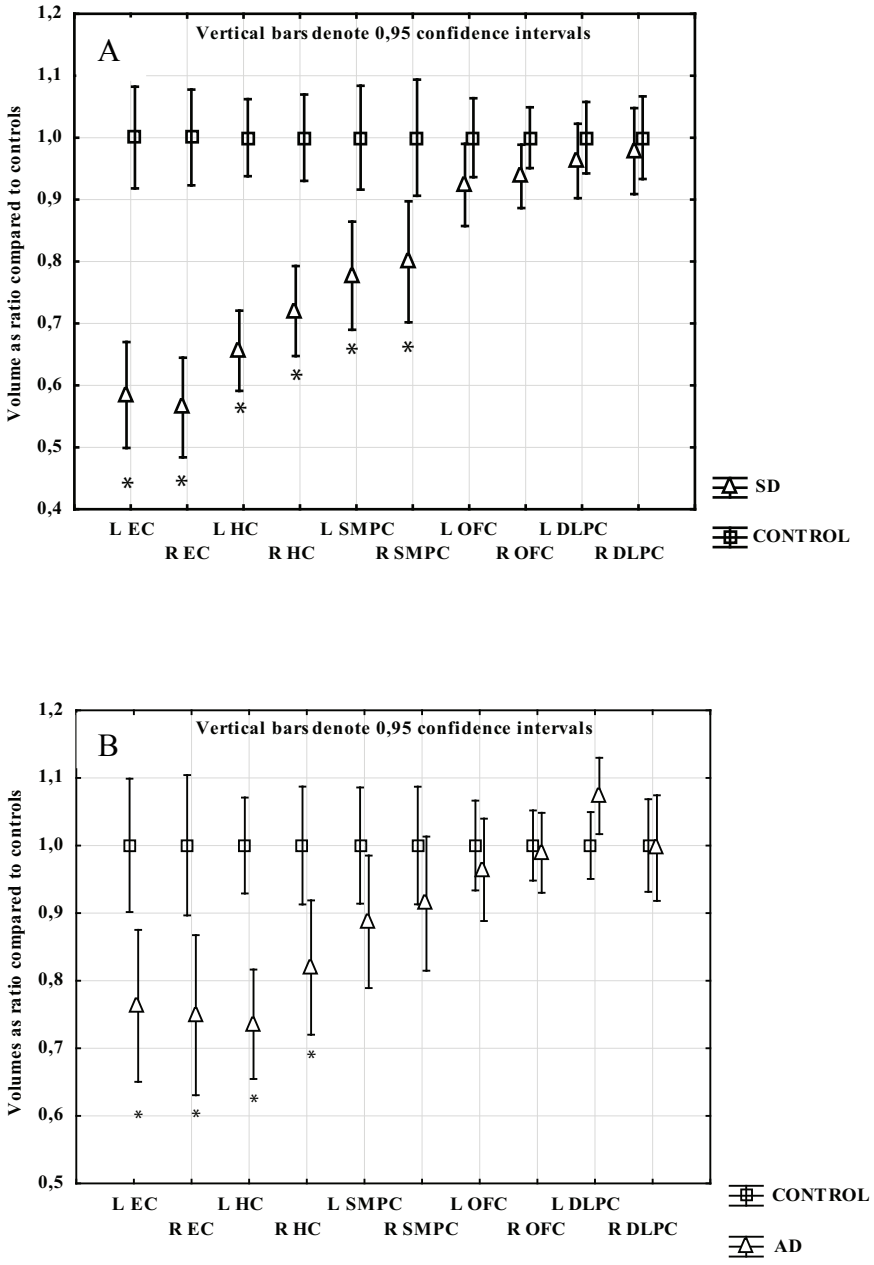

Figure 10
Volume loss in SD (A) and AD (B) compared to controls. The X-axis denotes measured regions. The Y-axis denotes the volume as the ratio compared to the volume of the controls (set to 1). The measured volumes are the entorhinal cortex (EC), the hippocampus (HC), the subcallosal ventromedial prefrontal cortex (SMPC), the orbitofrontal cortex (OFC) and the dorsolateral prefrontal cortex (DLPC). R: right, L: left. *: $p<0.01$ (unpublished data. For description of included patients see study III).

5 AIMS

5.1 AIM OF STUDY I

Patients with a neurodegenerative disease are primarily affected in specific brain networks, which is commonly reflected in a characteristic regional pattern of atrophy. Such network-specific atrophy patterns are furthermore generally correlated with a characteristic cluster of clinical symptoms. The aim of study I was to investigate the relationship between clinical symptoms and atrophy of the brain in subtypes of clinically diagnosed patients with frontotemporal lobar degeneration (FTLD).

5.2 AIM OF STUDY II

The aim of study II was to compare volumetric data on frontal lobe gyri acquired by manual tracing with data acquired by voxel-based morphometry (VBM).
The manual method uses sulci as landmarks for the gyri that are measured, while VBM uses templates to obtain data for the same gyri. Recent studies have shown that the relationship between cell structure and gross-morphology of the frontal lobe is weak. We therefore hypothesized that a template-based approach may be more rewarding in frontal regions than a manual method since the gross-morphological appearance of sulci may cause variance in volumetric data that is not related to an underlying cytoarchitectonic or functional region.

5.3 AIM OF STUDY III

The aim of study III was to compare the pattern of cortical atrophy in frontal and temporal regions with the pattern of hippocampal atrophic deformation in patients with FTLD and AD compared to controls.

5.4 AIM OF STUDY IV

Previous studies have shown that cortical regions of the frontal lobe may be particularly vulnerable to age-related processes; however data has been contradictory regarding the anterior part of the cingulate gyrus. The aim of study IV was to investigate age-related volume loss in the dorsal part of anterior cingulate gyrus in 505 normal elderly participants 60-97 years of age.

6 MATERIAL AND METHODS

6.1 SUBJECTS

6.1.1 Cohort I

Cohort I included healthy controls and patients with AD and FTLD. Participants were recruited retrospectively from the memory clinic at the Karolinska University Hospital Huddinge, Stockholm, Sweden. All participants went through the standard investigation procedure at the memory clinic (Andersson, 2007). Laboratory investigations for all subjects were done on blood, CSF and urine (including vitamin B12 measures, folic acid levels and thyroid function). Clinical diagnoses were determined at a multidisciplinary consensus conference with physicians, neuropsychologists, speech-language pathologists and nurses. FTLD syndromes were diagnosed according to international consensus criteria (Neary, et al., 1998). Patients with FTLD and AD at different stages of the disease were included. Diagnoses of AD were based on criteria of the International Classification of Diseases, Tenth Revision (ICD-10; World Health Organization., 1992).

The control group (CTL) was comprised of individuals referred to the memory clinic because of mild subjective forgetfulness in everyday life. Objective cognitive impairment was ruled out through comprehensive neuropsychological assessment (impairment was defined as performance 1.5 standard deviation unit below the age-normal mean on any cognitive test) (Wahlund et al., 2003). To further minimize the risk of including participants with neurodegenerative diseases in very early stages, we included only those participants whose performance did not deteriorate over a minimum of a 2-year follow-up. Background data included age at scanning, Mini-Mental State Examination (MMSE) score (Folstein, et al., 1975) and intracranial volume. Illness duration was also investigated by calculating the number of months/years between first indications of symptoms (in medical records) and the MRI investigation. A non-parametric Kruskal-Wallis ANOVA with a Mann-Whitney U test as *post hoc* was used for investigating differences in illness duration, age at scanning and MMSE scores.

6.1.2 Cohort II

Participants

The subjects included in the present MRI study are part of an epidemiological sample of 3363 people aged 60 years or older, participating in the Swedish National study on Aging and Care in Kungsholmen (SNAC-K). This is a longitudinal, multidisciplinary study on aging and health, initiated in 2001. SNAC-K was designed to detect the influence of lifetime genetic, environmental and biological factors on medical, psychological and social health in late adulthood. The SNAC-K population was stratified by age. Within each of the eleven pre-specified age cohorts (60, 66, 72, 78, 81, 84, 87, 90, 93, 96, 99+), persons were randomly selected to take part in the baseline examination. The baseline data collection includes information on present status and past events. The information has been collected through interviews, clinical examinations, and testing. The baseline data collection was completed in June 2004 and the follow-up data collection is ongoing. A subsample of 555 subjects was randomly selected from all non-institutionalized and non-disabled participants to undergo an MRI examination. On average, these 555 subjects were slightly younger, more educated and cognitively advantaged compared to the remaining sample. Subjects with severe cerebral diseases that directly affect the brain were excluded. Thus participants were excluded if they had: 1) Substantial degeneration or damage to the white matter (which in some cases could have been caused by stroke), 2) brain tumor, 3) alcohol addiction, 4) bipolar disorder, 5) Parkinson's disease, 6) epilepsy, or 7) a mini mental state examination (MMSE (Folstein et al., 1975)) score below 25.

After quality assessment of the baseline MRI images, 505 subjects (aged 60–97 years old; 300 females and 205 males) were finally included in this MRI study. Due to small sample sizes in the groups 81, 84, 87 and 87+ years of age, these four groups were combined into two groups: persons aged 81-84 years into "83" and persons above 86 years of age into "90". Thus, a total of six age groups (60, 66, 72, 78, 83, and 90 years) were used in the study.

Volumetric data of the HC and the ACC were acquired for 505 subjects, while the OFC was measured only for a subsample (n=124) evenly distributed between the age groups.

6.1.3 Subjects in study I-IV

Clinical data of participants from cohort I included in:

Study I

	Control	FTD	SD	PNFA
N	27	12	13	9
Sex (M:W)	7:20	3:10	5:9	3:6
Age (y)	61.1 (53-78)	59.5 (42-72)	63.8 (52-77)	64.9 (57-78)
MMSE	28.7 (25-30)	20.8 (10-30)+	22.9(5-29)+	22.5 (15-28)#
Disease duration (y)	-	1.7 (0.3-3.4)	3.9(1.3-7.7)&	3.6 (0.1 – 8.1)

FTD: frontotemporal dementia, SD: semantic dementia, PNFA: progressive nonfluent aphasia, M: men, W: women, MMSE: minimental state exame, , +, #, & Kruskal-Wallis test, + = $p<0.01$ compared to controls, # = $p<0.05$ compared to controls, & = $p<0.01$ compared to FTD.

Study II

	DACC	RACC	HC	DLPC	MMSE	AGE
AD	20	20	20	20	23	62
Controls	30	24	42	28	29	62
FTD	12	12	12	12	21	59
SD	12	12	12	12	23	64

The table includes number of subjects included for each regional comparison. DACC: dorsal anterior cingulate, RACC: rostral anterior cingulate, HC: hippocampus, DLPC: dorsolateral prefrontal cortex, MMSE: minimental state exam, AD: Alzheimer´s disease, FTD: frontotemporal dementia, SD: semantic dementia, AGE: mean age at scan.

Study III

Group	Age at scan	Illness duration	MMSE	N	M/F	ICV
CTL	63(53-78)		29(25-30)	21	7/14	1408(1116-1673)
AD	64(50-75)	2.5 (0.6-5.1)	22 (7-29)*	19	8/12	1384(1130-1648)
PNFA	65(57-78)	3.6 (0.1-8.1)	17 (0-28)*	9	3/6	1373(1296-1542)
SD	64(52-77)	3.9(1.3–7.7)	23 (5-29)*	13	5/8	1440(1204-1682)
FTD	60(42-72)	1.7 (0.3-3.4)	21 (10-30)*	13	4/9	1421(1138-1635)

CTL: controls. AD: Alzheimer's disease, FTD: Frontotemporal dementia, PNFA: Progressive nonfluent aphasia, SD: Semantic dementia, Mean (min-max) of: Age at scan, Illness duration, MMSE: mini-mental state examination, ICV: intracranial volume N: number of subjects. M/F: the number of males/females included in the study. * = significantly different from controls in Kruskal-Wallis ANOVA with a Mann-Whitney U-test post-hoc

Cohort II

Participants from the cohort included in study IV

Demographic characteristics of the whole sample of 505 subjects

	Main group	
	Female (n = 300)	Male (n = 205)
Variable	Mean (SD)	Mean (SD)
Age (years)	71.7 (8.9)	70.7 (9.1)
Education (years)***	11.9 (3.8)	13.5 (4.3)
ICV (cm^3)***	1402.72 (105.32)	1612 (130.31)
Total ACC (cm^3)	2.35 (0.55)	2.31 (0.57)
Total HC (cm^3)	6.49 (0.84)	6.98 (0.94)

There are gender differences *within* groups for variables marked with asterisks. *** $p < .001$ ACC: anterior cingulate HC: hippocampus, ICV: intracranial volume.

Demographic characteristics of the subsample of 124 subjects

	Female (n = 66)	Male (n = 58)
Variable	Mean (SD)	Mean (SD)
Age (years)	75.1 (10.4)	74.6 (9.8)
Education (years)***	11.6 (3.9)	13.9 (4.2)
ICV (cm^3)***	1402.34 (108.17)	1592.56 (107.72)
Total OFC (cm^3)***	24.12 (2.96)	26.43 (3.41)

There are gender differences *within* groups for variables marked with asterisks. *** $p < .001$, OFC: orbitofrontal cortex. ICV: intracranial volume.

Number of included subjects divided into age groups

AGE	OFC	HC & ACC
	W M	W M
60	13, 10	74, 65
66	10, 12	67, 47
72	9 , 9	53, 27
78	10 , 8	43, 28
83	13, 11	45, 25
90	11, 8	18, 13

Number of included subjects divided into age groups in the measured regions. M: men, W: women, OFC: orbitofrontal cortex, HC: hippocampus, ACC: anterior cingulate cortex.

6.2 PROCEDURES

6.2.1 Image acquisition

6.2.1.1 Study I, II and III

T1-weighted MRI scans were acquired on a 1.5 T Siemens Magnetom Vision Plus scanner (Siemens Medical Systems, Erlangen, Germany). A three-dimensional magnetization-prepared rapid gradient echo (3D-MPRAGE) pulse sequence (TR 11.4 ms; TE 4.4 ms; TI 300 ms; FA 10 º; NEX 1) was used to obtain 72 contiguous coronal 2.5 mm-slices with 512 × 144 matrix and 230-mm FOV.

6.2.1.2 Study IV

MRI scanning was undertaken on a 1.5T scanner (Philips Intera, Netherlands). 3D FFE (fast field echo) T1, axial SE (spin echo) PD/T2, axial FLAIR (fluid-attenuated inversion recovery) and axial DTI (diffusion tensor imaging) were acquired. In this study, the 3D FFE T1 images (TR =15ms, TE = 7ms, Flip angle = 5◦, number of slices = 128, thickness = 1.5mm, FOV = 240, matrix = 256x256) were used for volumetry.

6.2.2 Preprocessing, parcellation and volumetric measurements

6.2.2.1 Alignment

Images were aligned in the axial plane along a line drawn between the anterior and posterior (AC-PC) commissures for tracing of regions of interest, except for the entorhinal cortex and hippocampus in study I which was traced perpendicularly to the long axis of the left hippocampus on contiguous coronal slices.

6.2.2.2 Parcellation

The software MRIcro (Version 1.37; Roden and Brett, 2000) was used for parcellation of the cortex. When using this software, an image can be viewed in horizontal, sagittal and coronal directions simultaneously with a reconstruction of the surface of the brain. By putting a synchronized crossbar on a particular position of the surface or on any of the three orientations of the MR image, the crossbar simultaneously shows the same position in the other directions and on the surface.

6.2.2.3 Measurements

Actual measurements on contiguous coronal slices were performed on the HERMES MultiModality software package (Nuclear Diagnostics, Stockholm, Sweden). Intracranial volume was measured by stereology point-counting technique (Howard et al., 2003).

6.2.2.4 Rules for delineation

6.2.2.4.1 Study I

Established protocols were used for parcellation of the cortical regions as follows: Intracranial volume (Eritaia et al., 2000), prefrontal cortex and insula (Crespo-Facorro et al., 2000), temporal pole (Galton et al., 2001), entorhinal cortex (Goncharova et al., 2001), hippocampus (Jack, 1994), and anterior cingulate gyrus (McCormick et al., 2006). For the posterior border of dorsal anterior cingulate gyrus, however, we followed rules proposed by (Fornito et al., 2006) and stopped tracing one slice after the disappearance of the anterior commissure moving from anterior to posterior on coronal slices.

6.2.2.4.2 Study II

Manual and template-based volumetric data was obtained for five brain regions: the dorsolateral prefrontal cortex (DLPC), the rostral and dorsal part of the anterior cingulate gyrus (rostral ACC, dorsal ACC), the orbitofrontal cortex (OFC) and the hippocampus (HC). The manual parcellation method which relied on indirect landmarks of sulci and gyri was done following rules proposed by Suzuki et al. (2005) for the DLPC and McCormick et al., 2006; for the cingulate cortex). In brief, the medial border of the DLPC was the cingulate sulcus, the lateral border the inferior frontal gyrus, the posterior border the precentral sulcus and the anterior border the frontomarginal sulcus. Borders for the cingulate cortex were the cingulate and the callosal sulcus. The posterior border of the rostral anterior cingulate was the one slice anterior to the position where the forceps minor of corpus callosum first connects the two hemispheres. For the posterior border of the dorsal anterior cingulate we followed rules proposed by Fornito et al (2006) finishing one coronal slice posterior to the anterior commissure. For the tracing of the orbitofrontal cortex we followed rules proposed by Crespo-Facorro et al (2000). In coronal view the medial border at the most anterior end was the superior rostral sulcus. When the olfactory sulcus became visible it was used as the medial border. The lateral border was to the anterior frontomarginal sulcus, at the centre the lateral orbital sulcus and at in the most posterior section the orbitoinsular sulcus. Tracing ended when the medial orbitofrontal gyrus was no longer visible moving from anterior to posterior (Crespo-Facorro et al., 2000).

Manual measurement of the hippocampus was done following rules proposed by Malykhin (Malykhin et al., 2007). The hippocampus was included as quality control of the VBM methods. This region exhibits high reliability in manual tracing and relatively small anatomical variability compared to cortical regions. The intracranial volume (ICV) was obtained by using a stereologic point-counting technique comprising manual tracing of the ICV on every fourth section, following landmarks proposed by Eritaia et al. (2000).

Voxel-based morphometry (VBM)

Structural data was processed with FSL-VBM, a voxel-based morphometry style analysis (Ashburner et al., 2000; Good et al., 2001b) carried out with FSL 4.1 tools (Smith et al., 2004). The procedure used is as follows:

1) First, brain-extraction of T1 images was performed using BET (Smith, 2002). In this step brain was extracted from surrounding tissue.
2) Next, tissue-type segmentation was carried out using FAST4.1 (Zhang et al., 2001). This tool segments a 3D image of the brain into different tissue types (Grey Matter, White Matter, CSF, etc.), whilst also correcting for spatial intensity-variations.
3) The segmented grey-matter image was then aligned to MNI152 standard space using the affine registration tool FLIRT (Jenkinson and Smith, 2001; Jenkinson et al., 2002).
4) The resulting images were averaged to create a study-specific template (which thus is an average image of all included subjects).
5) Native grey-matter images (for each individual subject) were then non-linearly re-registered to the study specific template.
6) The registered segmented images were then smoothed with an isotropic Gaussian kernel with a sigma of 2 mm.
7) Grey matter masks for parcellation of the investigated brain regions were created by drawing on the study specific template (from step 4) generated by the FSL program (Figure 2). The masks were drawn for the five regions previously measured by manual tracing (Lindberg et al., 2009).
   The regional masks were applied to the smoothed gray matter (sigma = 2 mm) data of each subject with AFNI (open source software for neuroimaging data analysis, NIH NIfTI) to obtain the mean density of gray matter (GM) in the masked regions.

6.2.2.4.3 Study III

Volumetric analysis was performed using HERMES BMAP Morphy Display (Nuclear Diagnostics AB, Stockholm, Sweden). The hippocampus was measured following rules proposed by (Malykhin et al., 2007). Tracing was performed on coronal sections perpendicular to a line drawn through the anterior-posterior commissure. This protocol divides the hippocampus into hippocampal head (HH), body (HB) and tail (HT). The most posterior part of the HH was defined as the first slice in which the uncal apex was clearly visible. The superior border was the alveus, the uncal recess and the inferior horn of the lateral ventricle. The medial border was the inferior horn of the lateral ventricle or the white matter of the parahippocampal gyrus. Further to the anterior, the superior border of the HH was the amygdala. The fimbria was included as the

superomedial border of the HB. The white matter of the parahippocampal gyrus was used to separate the subiculum from the entorhinal cortex by an imaginary line along the HB to the quadrigeminal cistern. The lateral border was the inferior horn of the lateral ventricle or the adjacent white matter. The superior medial border was the quadrigeminal cistern. The anterior border of the HB was the last slice before the appearance of the uncus. The anterior border of the HT was the slice in which the fornix was seen in full profile, or was separated from the wall of the ventricle. As in the HB, the fimbria was included but not the fornix. The white matter of the fornix defined the superior and lateral border boundaries, and the white matter of the parahippocampal gyrus the inferior border. The medial border was the CSF of the quadrigeminal cistern.

6.2.2.4.4 Study IV

The dorsal anterior cingulate was traced on coronal sections. Tracing began from the anterior at the first slice in which the corpus callosum white matter connected the two hemispheres. The posterior border was one slice after the putamen became visible in coronal view. The cingulate sulcus was the superior border and the inferior border was the deepest point of the callosal sulcus. For the definition of the cingulate sulcus we followed rules proposed by (McCormick et al., 2006).

The orbitofrontal cortex was segmented following rules proposed in a previous study (Crespo-Facorro et al., 2000). In brief they were as follows: Lateral borders were frontomarginal sulcus at the anterior end, the lateral orbital sulcus at the intermediate part and the orbital insular sulcus at the posterior part. Medial borders were the olfactory sulcus more to the anterior (when the olfactory sulcus disappears) the superior rostral sulcus on the medial wall of the frontal lobe became medial border.

6.2.3 Statistics

6.2.3.1 Study I

Analysis of variance

Significant differences between individual variables were also identified by one way analysis of variance. Results were corrected for multiple comparisons by Bonferroni correction (using Statistica, version 7.1, Statsoft, Inc. Tulsa, OK, USA). A p-value < 0.05 was considered significant. Every individual volume measurement of an individual structure ($V_{ind,\,struct}$) was first normalized for intracranial volume by dividing the volume of each individual's structure (VLS) by the individual's intracranial volume (ICV):

$$V_{ind,struct} = \frac{VLS}{ICV} \quad (1)$$

The discriminant analysis

The pattern of atrophy was investigated by partial least-square discriminant analysis (PLS-DA), which is a supervised multivariate data analysis method that is part of the SIMCA software (Umetrics AD, Umeå, Sweden). The results from the PLS-DA analysis were visualized by plotting two principal components of the model against each other in a scatter plot. This plot illustrates the degree of separation accomplished by the components. Each point in the scatter plot represents one patient. Each principal component receives a Q^2 value that describes the statistical significance and the predictive power of that component. A Q^2 value > 0.05 is considered statistically significant.

Sensitivity and specificity were calculated from the predictions made by leave-one-out cross validation. This means that a number of parallel models are built. Each model leaves one individual out. The data from this individual is then introduced into the model which results in a predictive value. The theoretically correct predictive value of membership in group one = 1 and group two = 0. The cut-off value for the predictions is 0.5. This means that all individuals with a predictive value > 0.5 are classified into group one while individuals with a value less than 0.5 are classified into group two. Sensitivity and specificity were then calculated as follows: Sensitivity is the number of true positive predictions divided by the sum of the number of true positive predictions and the number of false negative predictions. Specificity is the number of true negative predictions divided by the sum of the number of true negative predictions and the number of false positive predictions.
The PLS-DA allows us to plot the structures according to their importance for separating the groups. Structures receive a VIP (variable of importance) value. Values >1 reflects that the structure is a factor involved above average in the separation of groups.

6.2.3.2 Study II

Analysis of variance

Statistical analysis was performed with Statistica 10 (StatSoft, Inc., 2011). Volumetric data were analyzed by one-way-analysis of variance with Tukey HSD post-hoc test. All volumetric data were normalized by intracranial volume (ICV) by the formula volume of region/intracranial volume. *P* values less than 0.05 were considered significant.

Consistency between methods

Consistency between the volume of region/intracranial volume (normalized as z-scores) from the MM method was compared with grey matter density (normalized as z-scores) by intra class correlation coefficients (ICC) (Shrout and Fleiss, 1979). Contrary to traditional correlation that operates on paired observations ICC operates on data structured as groups. ICC is traditionally used for investigating reliability of rater in MM.

The theoretical formula for ICC is:

$$ICC = \frac{\sigma^2(b)}{\sigma^2(b) + \sigma^2(w)} \quad (2)$$

where σ^2(w) is the pooled variance within subjects, and σ^2(b) is the variance of the trait between subjects (Equation 2).

6.2.3.3 Study III

Analysis of variance

Statistical analysis was performed with Statistica 10 (StatSoft, Inc., 2011). Volumetric data were analyzed by one-way-analysis of variance with Tukey HSD post-hoc test. All volumetric data were normalized by intracranial volume (ICV) using equation 1. *P* values less than 0.05 were considered significant.

Shape analysis

Shape analysis was performed in an automated fashion using the University of North Carolina shape analysis toolkit SPHARM (http://www.nitrc.org/projects/spharm-pdm). The method has previously been described in greater detail in (Styner et al., 2006). Segmented 3D binaries are initially processed to fill interior holes, ensure spherical topology and perform minimal smoothing. These are then mapped into spherical harmonic shape description (SPHARM-PDM), whereby the boundary surfaces of each shape are mapped under area-preservation onto a spherical parametrization, followed by describing the original surface locations via sets of coefficients weighting spherical harmonic basis functions (Brechbuhler et al., 1995). The correspondence between surfaces is established by parameter-based rotation, itself based on first-order expansion of the spherical harmonics, and is then uniformly sampled into a set of 1002 surface points. This surface is then aligned to a study-averaged template for each structure (left and right hippocampus) using rigid-body Procrustes alignment (Bookstein, 1997), with normalization for head size using an ICV based scaling factor f_i, where

$$f_i = \frac{\overline{ICV}}{ICV_i^{1/3}} \tag{3}$$

taken from (Styner et al., 2006). Here $\overline{ICV}$ is the mean ICV and ICV_i is the individual ICV value.

We then compute local non-parametric statistical tests that compares the local surface coordinates for group mean differences at the 1002 surface locations in order to compare shapes between groups (Levitt et al., 2009; Styner et al., 2006; Styner et al., 2007). A local group difference metric between groups of surface coordinates is derived from the Hotelling T^2 two-sample metric (Styner et al., 2006; Styner et al., 2007). As the shape analysis involves computing 1002 hypothesis tests, one per surface location, a correction for multiple testing is necessary, as an uncorrected analysis would be overly optimistic.

The shape analysis uses permutation tests for the computation of raw uncorrected p-values. A false discovery rate (FDR) correction (Genovese et al., 2002) is applied instead of a Bonferroni-based multiple comparisons correction, resulting in a less pessimistic control for type 1 errors and a less conservative estimate of false negatives (Styner et al., 2004). Shape statistical analysis significance maps showing local statistical p-values, raw and corrected for FDR, are generated. In the results only FDR corrected data are shown. A global shape difference is computed, summarizing average

group differences across the surface. Shape statistical analysis also provides visualizations of group test local effect size via mean difference magnitude displacement, which display the magnitude of deflation (mm) between the same point on the mean surface of group 1 and the mean surface of group 2, in a manner analogous to a vector map.

6.2.3.4 Study IV

Statistical analysis was performed using Statistica 10 (StatSoft, Inc. 2011). The volumetric data was analyzed by one-way-analysis and two-way analysis of variance with a Bonferroni post-hoc test. All volumetric analysis were performed on data that was normalized by intracranial volume (ICV) using equation 1.

Rate of volume loss between age groups

The volume loss in percent per year was calculated by comparing each individual volume with the mean of the nearest younger age-group according to the expression

$$V_{loss} = \frac{\bar{V}_{age,i-1} - V_{ind,i}}{\bar{V}_{age,i-1}(Age_{i,ind} - Age_{i-1})} \quad (4)$$

where V_{loss} is the percentual volume loss per year, $\bar{V}_{age,i-1}$ is the mean volume of the next younger age group, $V_{ind,i}$ is the individual volume in the age group, $Age_{i,ind}$ is the actual age of the individual and Age_{i-1} is the age of the next younger age group.Thus every individual volume at 66 was compared with the mean volume at 60, each individual at 72 with the mean at 66, at 78 with the mean of 72, at 83 with the mean of 78 and at 90 with the mean of 83. To calculate the deviation in percent per year, the results were divided by the number of years between the mean (for instance 60) and the individual´s age (66) which in this example equals 6. So in the comparison between the mean of 60 with the individual volume at 66 the expression was as follows:

((Mean volume of the 60 group – individual volume at 66)/Mean volume of the 60 group)/6

Finally the results of the described percentage calculations were combined into a young (60 years to 72 years of age) and an old (78 to 97 years of age) age-group.

Correlation

Pearson's correlation coefficient (*r)* was used to investigate the association between regional volume and age. For testing differences in the magnitude of the correlations Steiger's *Z* test was used. This test takes into account the strength of the association between the members of all relevant pairs of variables (Steiger, 1980). A prerequisite for Steiger's *Z* test is that the same subjects are included for all investigated regions. Thus for this test only the 124 subjects that had data available for all regions were included.

6.2.4 Ethics

All studies were approved by the Regional Ethical Review Board in Stockholm. Study I-III approved by (DNR: 2010/1817-31/2) and study IV by (DNR: 01-114).

7 RESULTS AND DISCUSSION

7.1 PAPER I

7.1.1 Results

The main hypothesis in study I was that the very specific symptoms displayed by the subtypes of FTD would correspond to distinct patterns of cortical atrophy. This hypothesis was generally confirmed. Three patterns could be identified.
FTD patients, who showed changes in personality and social behaviour, generally displayed more right-side frontal atrophy than other subtypes of FTLD. PNFA patients, with a progressive loss of speech, often displayed a predominance of left side atrophy both in frontal and temporal regions. Finally SD patients, with a progressive loss of word meaning, displayed more severe atrophy in the temporal regions, in particular in the anterior temporal lobe, than other subtypes of FTLD.

7.1.2 Discussion

The study of morphometric subclassification of patients with FTLD must, in retrospect, be seen in a historical perspective. When this work began, to our knowledge, only one study had investigated the pattern of cortical atrophy in all FTLD subtypes simultaneously (Grossman et al., 2004).
After this study was published there has been explosion in this field of research and hundreds of articles have been published on the volumetric characteristics of FTLD (e.g. Boxer et al., 2011; DeJesus-Hernandez et al., 2011; Galantucci et al., 2011; Gorno-Tempini et al., 2011; Kim et al., 2011; Rabinovici et al., 2008; Rabinovici and Miller, 2010; Rankin et al., 2009; Seeley et al., 2009; Tartaglia et al., 2011; Whitwell and Jack, 2005; Whitwell et al., 2011; Wilson et al., 2009; Wilson et al., 2010a; Wilson et al., 2010b) for reviews see (Rabinovici and Miller, 2010; Whitwell and Jack, 2005).

Maybe one of the most important recent insights is that FTD and PNFA but not SD patients may display the clinical symptoms of FTLD without having detectable atrophy on a structural MRI scan (Davies et al., 2006; Kipps et al., 2007). In our case we did not have any patients with normal appearance on the MRI scans, which thus may explain the very high degree of specificity and sensitivity we found in the comparison between the different variants of FTLD and in the comparison between FTLD patients and control subjects.

7.1.3 Conclusions

In light of new evidence our previous conclusions could thus be modified as follows: When an atrophic pattern is *detectable* in patients with FTLD, then this pattern is generally characteristic for each FTLD subtype. This emphasizes that the clinical

symptoms displayed in FTLD are related to pathology or atrophy of specific cortical networks, which may be manifested in subtype-specific patterns of atrophy (Lindberg et al., 2009).

7.2 PAPER II

7.2.1 Results

The main finding of study II was that there relatively good consistency between data generated by manual tracing and data generated by voxel-based morphometry for the orbitofrontal cortex, the dorsolateral prefrontal cortex and the hippocampus. For the anterior cingulate cortex, however, the consistency between these methods was very poor. Another important finding was that data on the anterior cingulate generated by VBM was more consistent with findings in previous studies on the investigated subtypes of dementia.

7.2.2 Discussion

Study I showed that each clinical subtype of FTLD generally displays a characteristic pattern of atrophy which can be related to the specific symptoms of each subtype. From a methodological point of view it could thus be said that the manual tracing method generated volumetric data that successfully could describe these patterns.
One problematic aspect was, however, that while the manual method generated data that could describe the large-scale pattern of atrophy for each subtype of FTLD, it was not successful at all in describing regional pattern of atrophy in some individual cortical regions. For example, previous studies have indicated that the anterior cingulate gyrus may be more atrophic in FTD than in other subtypes of FTLD, and the inferior frontal gyrus should according to literature be particularly atrophic in PNFA. This could not be confirmed in study I.

Thus the fundamental question was why the manual method was successful in describing atrophy in large cortical regions as well as in large scale patterns of atrophy in a combination of cortical regions while the method was less sensitive for detecting atrophy in small cortical regions.

A possible explanation for this discrepancy between VBM and manual tracing for small cortical regions may be found in the results of a previous study that investigated the reliability of cortical sulci and gyri as landmarks for cytoarchitectonic cortical areas (Fischl et al., 2008). Interestingly this study found that while sulci were relatively reliable landmarks for primary or unimodal cortical areas, they were highly unreliable for multimodal areas of the cortex. A sulcus was on average found to deviate with up to 1 cm from cytoarchitectonic areas in some parts of the frontal lobe.

Thus the sulci- and gyri- based parcellation performed in study I may have been reliable in describing the size of a cortical gyrus, while it was unreliable in predicting or estimating the volume of cytoarchitectonic regions.

We hypothesized that a template-based approach that does not consider the individual appearance of sulci and gyri would perform better than manual tracing, when comparing results with previous studies on the same variants of dementia.

The reason for this hypothesis was that while both manual tracing and VBM may be equally poor in predicting cytoarchitecture, the manual method will add further variance in the volumetric data caused by the by anatomical variability of sulci and gyri.

We furthermore hypothesized that the effect of the morphological variability of sulci and gyri would be related to the size of the region investigated. If we assume that sulci would do equally poorly in predicting the location of any multimodal frontal lobe region, then a mean deviation around 1 cm from cytoarchitecture may be a reasonable estimation (Fischl et al., 2008). The relative effect of anatomical variability would thus, in percent, be much larger for a small cortical region than a large.

The results of study II confirmed these two hypotheses. VBM thus produced data on the anterior cingulate that was more in line with the findings of previous studies. The results from VBM were furthermore much more consistent with the results from manual tracing in large cortical regions than in the small subparts of anterior cingulate.

7.2.3 Conclusions

These results of study II suggest that manual tracing following the individual anatomy of sulci and gyri may be problematic in small multimodal regions of the frontal lobe. In such cases, a template-based approach may be more rewarding as it does not add further unrelated variance (caused by variation in gyral size) to volumetric results.

7.3 PAPER III

7.3.1 Results

The results of study III indicated that, in line with what was previously shown for cortical regions, the hippocampus has a specific pattern of atrophic deformation in each subtype of FTLD and that these patterns are partly different from the atrophic deformation found in AD. AD displayed proportionally more atrophic deformation of the hippocampal body, while FTLD had more or equal amount of atrophy in the hippocampal head.

The local shape deformation of the hippocampus was interpreted using an anatomical atlas as a reference (Duvernoy, 2005). Based on a comparison of the location of deformation with the anatomical atlas we estimated which hippocampal subfields that that may be the most affected in FTLD and AD. The location of the deformation of hippocampus both in FTLD as well as in AD indicated that subiculum as well as cornu ammonis 1 (CA1) may be particularly vulnerable hippocampal subfields in both variants of dementia.

7.3.2 Discussion

Study III has shown that the subtypes of FTLD have three different patterns of deformation in the hippocampus which also are different from the deformation seen in AD. This could be discussed from three perspectives:

1. In relation to cortical atrophy.
2. In relation to the clinical symptoms displayed by each subtype of dementia.
3. In relation to the potential pathology that that is causing the neurodegenerative disease.

7.3.2.1 The atrophic deformation of hippocampus in relation to the pattern of atrophy in cortical regions

Study I showed that each subtype of FTLD had a characteristic pattern of cortical atrophy. We also found some common characteristics in the FTLD subtypes, such as the anterior parts of cortical regions often being more atrophic than the posterior parts. Thus were the anterior frontal and temporal lobes more atrophic than the posterior parts of these lobes in both FTD and in PNFA, while only the temporal lobe displayed this pattern in SD. As in the cortex, all the FTLD subtypes were proportionally more affected in the anterior than the posterior part of the hippocampus. AD was on the other hand more affected in the middle part of the structure (the hippocampal body).
Figure 11 displays the shape differences between SD and AD in the left hippocampus. The 3D image illustrates the hippocampus from above.

Lateral

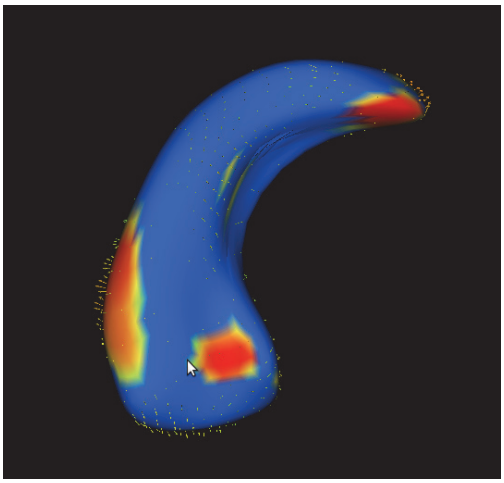

Medial

Anterior

Figure 11

The statistical shape maps display the significance of local deformations (SD<AD).
Warmer colors on the structure refer to smaller *P*-values (less than 0.05). Blue color corresponds to *P*-values above 0.05. Displacements are illustrated by the small arrows on the hippocampal surface (unpublished results).

7.3.2.2 Hippocampal deformation in relation to clinical symptoms

As this study did not involve any formal behavioral test, comments about the relevance of the distribution of hippocampal atrophy for emotional behavior are admittedly speculative, yet does indicate possibilities for further research. It can be noted that particularly FTD and SD displayed proportionally more anterior atrophy than PNFA and AD. As discussed in the introduction, the anterior parts of hippocampus are associated with emotional processing (Fanselow and Dong, 2010). It is interesting to note that the international consensus criteria for FTLD describe alteration in emotional behavior both in SD ("loss of sympathy and empathy") and FTD ("decline in social interpersonal conduct"), while PNFA is defined by having "early preservation of social skills" (Neary et al., 1998). Furthermore, the DSM-IV-R does not include emotional or social dysfunction as diagnostic criteria for AD (American Psychiatric Association, 2000). Thus the two dementia types that displayed largest anterior hippocampal atrophy in this study have been described as developing emotional and social dysfunctions. Whether the anterior hippocampus by itself may be relevant for these changes cannot, however, be investigated in our data. Atrophy of this region could for example also be an indirect indicator of a more general atrophy of the anterior temporal lobe (including the amygdala and the temporal pole).

In previous studies on the frontal and temporal cortex it has been shown that patients that display atrophy on the right side are more prone to display behavioral dysfunctions than patients with atrophy on the left side (Miller et al., 1993; Rosen et al., 2005; Seeley et al., 2005).

Our study found more involvement of the posterior part of hippocampus in AD, which potentially could affect the hippocampal memory system, while we found more involvement of the right anterior hippocampus in FTD and SD, which thus could affect the cortical system that is responsible for regulating emotions. In figure 12 we compare the degree of atrophy in the hippocampal head with the degree of atrophy in the hippocampal tail. Note that both FTD and SD have proportionally more atrophy in the hippocampal head than in the tail, while AD have approximately the same degree of atrophy in the head and the tail.

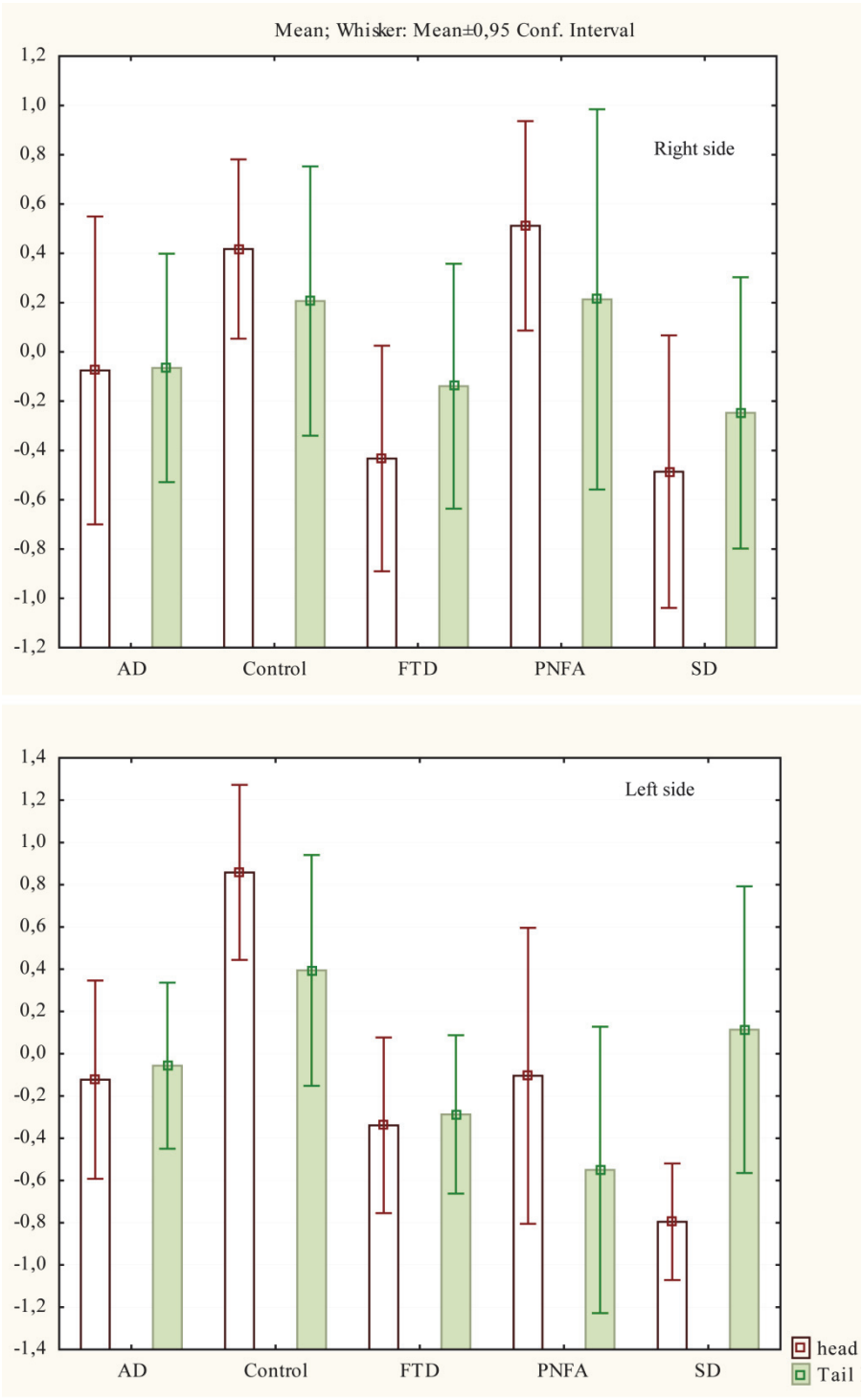

Figure 12

Relative degree of atrophy in the most anterior part (the head) and most posterior part (the tail) of left and right hippocampus. The Y-axix shows the volume of the subparts presented as ratio (volume of structure/intracranial volume) normalized as z-scores.

7.3.2.3 *Atrophy in relation to pathology*

While each subtype of dementia displayed a partly unique pattern of hippocampal deformation, we also found more similarities between some variants of dementia than between others. The most striking similarity was found between patients with AD and PNFA. A previous study has shown that a substantial number of patients that display the symptoms of PNFA may at postmortem be classified as AD (Alladi et al., 2007). This could thus potentially explain the similarity between AD and PNFA in the deformation of hippocampus.

7.3.3 Conclusions

This study suggests that both the FTLD subtypes and AD are most vulnerable to atrophy in CA1 and the subiculum. In contrast to FTLD, AD displayed proportionally more atrophy of the HB than the HH. FTD only displayed atrophy in the HH, while SD displayed atrophy of the whole hippocampus. There was some resemblance in the pattern of hippocampal deformation between AD and PNFA. This may potentially reflect the fact that patients with the clinical diagnosis of PNFA more often display AD pathology than other FTLD subtypes.

7.4 PAPER IV

7.4.1 Results

Anterior cingulate gyrus

The main finding of study IV was that the dorsal part of the anterior cingulate gyrus displayed very limited age-related volume loss. Only women at 90 years of age had significantly smaller volume than 60-year-old women. No difference between age groups was found in men. In a previous study we have shown that the hippocampal formation was relatively unaffected by age-related volume loss until the age of 72. After the age of 72 there was a relatively fast decrease of volume in this region (Zhang et al., 2010).

7.4.2 Discussion

The relative preservation of the dorsal anterior cingulate is consistent with the “last in (last to mature), first out (first to show age-related volume loss) hypothesis”. The anterior cingulate has been shown to mature earlier than the prefrontal cortex (Casey et al., 2005; Westlye et al., 2010b). One study suggests that the prefrontal cortex displays largest age-related volume loss in the age of 30-60, while volume loss in unimodal and paralimbic regions may occur later in old age. We found more age-related volume loss

in both the hippocampus and in the anterior cingulate after age 72. However when we compared the young (60-72 years) with the old (78-97 years) participants, the correlation between regional volume and age was significantly higher in the old interval in the hippocampus but not in the anterior cingulate. This thus indicates that the anterior cingulate may be remarkably preserved both in comparison with regions of the prefrontal cortex as well as in comparison with another limbic region.

7.4.3 Conclusions

This study demonstrates that the grey matter of the dorsal anterior cingulate cortex may be selectively preserved at old and very old age, both in comparison to another region of the limbic system, and to another region in the frontal lobe. Age-related shrinkage may thus differentially affect regions of the frontal lobe as well as regions within the limbic system.

8 GENERAL CONCLUSION OF THE THESIS

The four studies of this thesis have shown that regional volume loss in the brain is generally more pronounced in a degenerative disease, such as FTLD or AD, than in normal age-matched elderly subjects. We have further shown that pathological loss of volume commonly affects specific brain networks depending on what type or subtype of degenerative disease the patient is suffering from. We found that this network-specific neurodegeneration of cortical and sub-cortical brain regions often is reflected in characteristic clusters of clinical symptoms.

A problem in cortical volumetric studies is that the size of a single gyrus may not reflect the size of an underlying functional or cyto-architectonic area. We have shown that the calculation of the mean amount of cortical grey matter in the estimated location of a cortical region, such as the anterior cingulate gyrus, may be more sensitive to pathological volume loss than the actual volume of the same gyrus.

Finally this study has demonstrated that normal aging is associated with volume loss of cortical regions in the frontal lobe. As previously shown we furthermore confirm that volume loss is more severe in prefrontal regions, such as the orbitofrontal cortex, than in limbic regions such as the anterior cingulate gyrus.

9 ACKNOWLEDGEMENTS

It has been a great privilege to have the opportunity to write this thesis. The Karolinska institute (KI) provides a fantastic environment, not only for research in medicine, but for the academic process in general. It has occurred to me over and over again that I am surrounded by very bright people! And I am very happy to acknowledge:

Lars-Olof Wahlund, my main supervisor. Lars-Olof has given me the opportunity to work in this environment that I treasure so highly. He has furthermore taken on the difficult task of making my writing (not to speak of my figures and tables) comprehensible to other people than myself. I wonder how many times Lars-Olof read and corrected my first manuscript? As a supervisor Lars-Olof has given me very much liberty to test and work with different volumetric methods. Lars-Olof provides a truly liberal research environment in his lab, which allows each student to work and write in his or her own style.

Mussie Msghina. Mussie has, as co-supervisor, been a good discussion partner several times during my PhD work. His great knowledge of the frontal lobe and psychiatric syndromes has often been very useful. He has several times provided me with additional clues on how to interpret data I have been working on.

Per Julin. Per has extensive knowledge of image processing, and he has as co-supervisor provided me with good advice on the technical use of different image-processing tools.

Eric Westman. I have known Eric now for quite some time and have many times been impressed by his competence, particularly his broad knowledge that encompasses so many aspects of research in the MR-field.
While I may have been the "manual tracing" guy in our lab since my tutor Yi Zhang left, Eric was actually the first guy introducing me to the manual volumetric method. At the animal camera at KI Solna he showed me how to trace mouse hippocampus in strange software called Amira.
Eric has after his own dissertation taken on a role in our lab supporting other researchers at all levels. He has also been a very good reviewer and co-author of my last papers. His multivariate methods keep popping up like mushrooms in different posters from our department at international conferences. I am confident that I in 10 years time will have to address him as professor Westman!

Yi Zhang. I consider Yi to be my tutor in manual tracing. We have had a lot of fun in Imagelab and I was sorry that Yi left after finishing his thesis. I particularly missed Yi´s philosophical reflections on things and life. The first time I was working in Imagelab (with my mouse images) a very silent Chinese guy was sitting beside me, measuring the entorhinal cortex. Having no knowledge about Unix I managed to mess up the lab computer several times. I got rather irritated and I said out loud: "I need a rest!". Yi looked up and said: "Yes, computer needs rest too!"

Per Östberg. Per has been a constant reviewer of my writing, and the quality of my text, no doubt, would have been much poorer without his contributions.
Per's language skills are truly impressive but he also has extensive knowledge about frontotemporal dementia. Per´s contribution to my work on this thesis has been so

important that I "post-hoc" would like to call him my forth supervisor. One funny thing is that no matter how well I try to research the topic I am writing on, Per always manages to find a reference that was written 50 years earlier than the one I found.

Martin Holmberg. I first met Martin in high-school more than 30 years ago. I myself was probably the worst student in my class, while Martin, no doubt, was one of the brightest. There were a lot of discussions on politics in high school. I was myself a very left-winged man, while Martin was rather blue, supporting "free competition good for Sweden". We were probably rather simple-minded at that age. However one could have thought that Martin´s political view would make him "fly as a rocket" leaving me and other less clever students far behind. Instead he frequently sat beside me (particularly during math lessons) trying to make me understand some problems that I could not figure out. During the work on my PhD project Martin has yet again been a patient tutor. This time, however, I have had the opportunity to learn from his knowledge on writing. Working in the medical business, Martin is also an excellent reviewer of medical research.

Carl-Henrik Ehrenkrona. Carl-Henrik is attending the psychology program at the Karolinska Institute. A couple of years ago Carl-Henrik started to work extra at the Imagelab to help me measure structures of the brain in the large SNACK-project. He was training for a couple of months and managed to acquire the skills of manual tracing. Carl-Henrik is a very bright young man and he no doubt taught me a much as I taught him. Carl-Henrik has impressed me with his broad knowledge. I am confident that he can do anything he wants in research.

Eva Örndahl. Eva has taken the difficult task of administrating Image lab /SMILE. She has furthermore been a good reviewer of my recent text, including the so called "kappa" in this thesis (in which she has been tireless in scrutinizing every sentence and every word of the text).The arguments and readability of this text have no doubt been improved by her sharp eye for details.

Anette Eidehall. Anette had bravely mastered the task of administratively keeping track of me. I do not think anyone envies her this task but, as far I can tell, she has mastered it without the aid of chemical substances (such as valium or anti-depressants). For this, she has my admiration!

Leif Svensson. Leif has been a great supporter when I have run into trouble with the software "Hermes" that I used in some of my earlier studies at SMILE. He has also been kind enough to tailor-make applications used by me.
Even though software's are best when they are working – it has been great fun to "bother" Leif when something has gone wrong. First of all he always has a fitting comment on my activity in relation to the problem at hand. For example one time I managed to jam the computer by putting in too many images. Leif noted: "Yes, though I am surprised that you did not put in all the images" (in this context, all was equal to about 6000 images). One time my wife was visiting Imagelab. Working in the lab I suddenly heard her and Leif (from the coffee room beside the lab) comparing the messes I was creating at home with the ones I was creating on Imagelab´s computers. Apart from all the fitting comments on my activities Leif has also been a very intelligent and sensible discussion partner. The neuro-image community is greatly influenced by some of the major softwares used for image analysis. Some methodological concepts are almost taken for granted. In discussions with Leif I have

several times realized that some of these concepts may have a completely different meaning if circumstances are altered.

Gabriela Spulber. Gabriela started her PhD studies at about the same time as I did. We have in a way been representing two opposite sides to volumetric research in our lab. If I have been Mr. Manual Tracing, Gabriela has indeed been Ms. Automatic Volumetric Methods. Gabriela has been a good discussion partner and we have from time to time had the opportunity to discuss the outcome of different volumetric approaches.

Abdul Mohammed. Abdul gave me the opportunity to do my research preparatory course in neuroscience in his lab, even if I did not have any previous knowledge in research in the medical field.

Nenad Bogdanovic. Nenad allowed me to practice staining methods in his lab. He has furthermore provided me with good advice when working with volumetric measurements on MRI:s.

Johanna Öberg. Johanna was a good contributor to my first paper, helping me to run the multivariate statistics.

Eva-Lena Engman and Lisa Botes. Eva-Lena and Lisa are former administrators of Imagelab. Both of them have been great supporters of my own and other users' activities in Imagelab.

The rest of the people in Lars-Olof´s lab. Lately many new bright talents have joined our lab, including Amir Manzouri, Carlos Aguilar and Soheil Damangir and Raffaella Crinelli. All of them have contributed to my knowledge on new volumetric softwares that can be used to analyze MRimages of the brain.
There seems to be no computer question that Carlos cannot answer. Amir have, by his programming skills, made it possible to run automatic analysis on images that I long ago deemed to be impossible to analyze using automatic softwares.

Tomas Jonssonand Tie-Qiang Li. T&T are experts in scripting and automatic image-processing at the department of medical physics. Both have several times provided me with good advice on how to script or analyze images automatically.

Neshat Lindberg. It is not an easy task to write papers for a PhD-thesis. And it does not become easier when one has to keep track of two relatively small children during the process. Thus some periods I stopped keeping track of them – leaving my wife with the task of juggling her own work and keeping track of my children's activities all by her self – poor her! And poor me …. that has to make it up to hear when this is over!

Mina and Sara Lindberg. My children Mina och Sara has helped me by not allowing me to be too depressed when wicked reviewers rejected my work. At such time it is easy to become depressed. Sara and Mina have, however, helped me to keep in mind the fundamentals of life, like sweeties for "Fredagsmys" or to play "kiss och bajs-spelet".

Håkan Magnusson. Håkan is my oldest friend and, as he himself tend to point out, he tend to be involved in all activities initiated by the Lindberg family – no matter if it is rebuilding the upper floor of our summer house, being "best-man" at our wedding, or just drinking wine or whisky at some party in our summer house. To keep with the

tradition Håkan had the “pleasant experience” of reading this thesis and provide comments – and his points was well taken! The best contribution has though been that we have had a lot of fun outside work – which has helped keeping the “equilibrium” of the authors mind.

This research has made use of the SMILE medical imaging laboratory at Karolinska University Hospital and Karolinska Institute, Stockholm, Sweden.

This work was supported by:

Foundation ”Gamla tjänarinnor”.

Foundation ”Ragnhild och Einar Lundströms Minne”.

Svenska Alzheimer fonden

10 REFERENCES

Abe, M., Hanakawa, T., Takayama, Y., Kuroki, C., Ogawa, S., Fukuyama, H., 2007. Functional coupling of human prefrontal and premotor areas during cognitive manipulation. J Neurosci. 27**,** 3429-38.

Agosta, F., Scola, E., Canu, E., Marcone, A., Magnani, G., Sarro, L., Copetti, M., Caso, F., Cerami, C., Comi, G., Cappa, S.F., Falini, A., Filippi, M., 2011. White Matter Damage in Frontotemporal Lobar Degeneration Spectrum. Cereb Cortex.

Alladi, S., Xuereb, J., Bak, T., Nestor, P., Knibb, J., Patterson, K., Hodges, J.R., 2007. Focal cortical presentations of Alzheimer's disease. Brain. 130**,** 2636-45.

American_Psychiatric_Association, 2000. Diagnostic and statistical manual of mental disorders, Vol., Washington, DC.

Amunts, K., Schleicher, A., Zilles, K., 2007. Cytoarchitecture of the cerebral cortex--more than localization. Neuroimage. 37**,** 1061-5; discussion 1066-8.

Andersson, C., 2007. Predictors of cognitive decline in memory clinic patients. Vol., ed.^eds. Karolinska institut.

Ashburner, J., Andersson, J.L., Friston, K.J., 2000. Image registration using a symmetric prior--in three dimensions. Hum Brain Mapp. 9**,** 212-25.

Baldo, J.V., Wilkins, D.P., Ogar, J., Willock, S., Dronkers, N.F., 2011. Role of the precentral gyrus of the insula in complex articulation. Cortex. 47**,** 800-7.

Barbas, H., Blatt, G.J., 1995. Topographically specific hippocampal projections target functionally distinct prefrontal areas in the rhesus monkey. Hippocampus. 5**,** 511-33.

Barbas, H., 2000. Connections underlying the synthesis of cognition, memory, and emotion in primate prefrontal cortices. Brain Res Bull. 52**,** 319-30.

Barbas, H., Zikopoulos, B., 2007. The prefrontal cortex and flexible behavior. Neuroscientist. 13**,** 532-45.

Bennett, D.S., Bendersky, M., Lewis, M., 2005. Antecedents of emotion knowledge: Predictors of individual differences in young children. Cogn Emot. 19**,** 375-396.

Bennett, M.R., Hacker, P.M., 2005. Emotion and cortical-subcortical function: conceptual developments. Prog Neurobiol. 75**,** 29-52.

Binney, R.J., Embleton, K.V., Jefferies, E., Parker, G.J., Ralph, M.A., 2010. The ventral and inferolateral aspects of the anterior temporal lobe are crucial in semantic memory: evidence from a novel direct comparison of distortion-corrected fMRI, rTMS, and semantic dementia. Cereb Cortex. 20**,** 2728-38.

Bliss, T.V., Collingridge, G.L., 1993. A synaptic model of memory: long-term potentiation in the hippocampus. Nature. 361**,** 31-9.

Bohland, J.W., Guenther, F.H., 2006. An fMRI investigation of syllable sequence production. Neuroimage. 32**,** 821-41.

Bookstein, F.L., 1997. Shape and the information in medical images: a decade of the morphometric synthesis. Computer Vision and Image Understanding. 97–118.

Boxer, A.L., Mackenzie, I.R., Boeve, B.F., Baker, M., Seeley, W.W., Crook, R., Feldman, H., Hsiung, G.Y., Rutherford, N., Laluz, V., Whitwell, J., Foti, D., McDade, E., Molano, J., Karydas, A., Wojtas, A., Goldman, J., Mirsky, J., Sengdy, P., Dearmond, S., Miller, B.L., Rademakers, R., 2011. Clinical, neuroimaging and neuropathological features of a new chromosome 9p-linked FTD-ALS family. J Neurol Neurosurg Psychiatry. 82**,** 196-203.

Braak, H., Braak, E., Yilmazer, D., de Vos, R.A., Jansen, E.N., Bohl, J., 1996. Pattern of brain destruction in Parkinson's and Alzheimer's diseases. J Neural Transm. 103**,** 455-90.

Brechbuhler, C., Gerig, G., Kubler, O., 1995. Parametrization of closed surfaces for 3-D shape description. Computer Vision, Graphics, Image Processing.

Broca, P., 1861. Remarks on the Seat of the Faculty of Articulated Language, Following an Observation of Aphemia (Loss of Speech). Bulletin de la Société Anatomique. 6**,** 330-357.

Brodmann, K., 1909. Vergleichende Lokalisationslehre der Großhirnrinde in ihren Prinzipien dargestellt auf Grund des Zellenbaues., Vol., Barth, Leipzig.
Buckley, M.J., Mansouri, F.A., Hoda, H., Mahboubi, M., Browning, P.G., Kwok, S.C., Phillips, A., Tanaka, K., 2009. Dissociable components of rule-guided behavior depend on distinct medial and prefrontal regions. Science. 325**,** 52-8.
Burzynska, A.Z., Nagel, I.E., Preuschhof, C., Gluth, S., Backman, L., Li, S.C., Lindenberger, U., Heekeren, H.R., 2011. Cortical thickness is linked to executive functioning in adulthood and aging. Hum Brain Mapp.
Casey, B.J., Tottenham, N., Liston, C., Durston, S., 2005. Imaging the developing brain: what have we learned about cognitive development? Trends Cogn Sci. 9**,** 104-10.
Catani, M., Howard, R.J., Pajevic, S., Jones, D.K., 2002. Virtual in vivo interactive dissection of white matter fasciculi in the human brain. Neuroimage. 17**,** 77-94.
Coles, J., Oomman, S.K., Henne, W.M., Bliss, R.M., Hoffman, T.C., Finckbone, V., Strahlendorf, H., Strahlendorf, J., 2008. AMPA-induced dark cell degeneration is associated with activation of caspases in pyramidal neurons of the rat hippocampus. Neurosci Lett. 436**,** 294-9.
Convit, A., Wolf, O.T., de Leon, M.J., Patalinjug, M., Kandil, E., Caraos, C., Scherer, A., Saint Louis, L.A., Cancro, R., 2001. Volumetric analysis of the pre-frontal regions: findings in aging and schizophrenia. Psychiatry Res. 107**,** 61-73.
Corbetta, M., Kincade, J.M., Shulman, G.L., 2002. Neural systems for visual orienting and their relationships to spatial working memory. J Cogn Neurosci. 14**,** 508-23.
Crespo-Facorro, B., Kim, J., Andreasen, N.C., Spinks, R., O'Leary, D.S., Bockholt, H.J., Harris, G., Magnotta, V.A., 2000. Cerebral cortex: a topographic segmentation method using magnetic resonance imaging. Psychiatry Res. 100**,** 97-126.
Dale, A.M., Fischl, B., Sereno, M.I., 1999. Cortical surface-based analysis. I. Segmentation and surface reconstruction. Neuroimage. 9**,** 179-94.
Dale, P., Augustine, G., Fitzpatrick, D., Hall, W., MacNamare J, White, L.E., 2008. Neuroscience, Vol., Sinauer Associates.
Damasio, A.R., 1996. The somatic marker hypothesis and the possible functions of the prefrontal cortex. Philos Trans R Soc Lond B Biol Sci. 351**,** 1413-20.
Davies, R.R., Kipps, C.M., Mitchell, J., Kril, J.J., Halliday, G.M., Hodges, J.R., 2006. Progression in frontotemporal dementia: identifying a benign behavioral variant by magnetic resonance imaging. Arch Neurol. 63**,** 1627-31.
Davis, S.W., Dennis, N.A., Buchler, N.G., White, L.E., Madden, D.J., Cabeza, R., 2009. Assessing the effects of age on long white matter tracts using diffusion tensor tractography. Neuroimage. 46**,** 530-41.
De Lacoste, M.C., White, C.L., 3rd, 1993. The role of cortical connectivity in Alzheimer's disease pathogenesis: a review and model system. Neurobiol Aging. 14**,** 1-16.
DeJesus-Hernandez, M., Mackenzie, I.R., Boeve, B.F., Boxer, A.L., Baker, M., Rutherford, N.J., Nicholson, A.M., Finch, N.A., Flynn, H., Adamson, J., Kouri, N., Wojtas, A., Sengdy, P., Hsiung, G.Y., Karydas, A., Seeley, W.W., Josephs, K.A., Coppola, G., Geschwind, D.H., Wszolek, Z.K., Feldman, H., Knopman, D.S., Petersen, R.C., Miller, B.L., Dickson, D.W., Boylan, K.B., Graff-Radford, N.R., Rademakers, R., 2011. Expanded GGGGCC hexanucleotide repeat in noncoding region of C9ORF72 causes chromosome 9p-linked FTD and ALS. Neuron. 72**,** 245-56.
Dombrowski, S.M., Hilgetag, C.C., Barbas, H., 2001. Quantitative architecture distinguishes prefrontal cortical systems in the rhesus monkey. Cereb Cortex. 11**,** 975-88.
Duvernoy, H.M., 2005. The human hippocampus : functional anatomy, vascularization, and serial sections with MRI, Vol., Springer, Berlin ; New York.
Elderkin-Thompson, V., Hellemann, G., Pham, D., Kumar, A., 2009. Prefrontal brain morphology and executive function in healthy and depressed elderly. Int J Geriatr Psychiatry. 24**,** 459-68.

Eritaia, J., Wood, S.J., Stuart, G.W., Bridle, N., Dudgeon, P., Maruff, P., Velakoulis, D., Pantelis, C., 2000. An optimized method for estimating intracranial volume from magnetic resonance images. Magn Reson Med. 44**,** 973-7.
Errington, M.L., Galley, P.T., Bliss, T.V., 2003. Long-term potentiation in the dentate gyrus of the anaesthetized rat is accompanied by an increase in extracellular glutamate: real-time measurements using a novel dialysis electrode. Philos Trans R Soc Lond B Biol Sci. 358**,** 675-87.
Fanselow, M.S., Dong, H.W., 2010. Are the dorsal and ventral hippocampus functionally distinct structures? Neuron. 65**,** 7-19.
Fischl, B., Sereno, M.I., Dale, A.M., 1999. Cortical surface-based analysis. II: Inflation, flattening, and a surface-based coordinate system. Neuroimage. 9**,** 195-207.
Fischl, B., Rajendran, N., Busa, E., Augustinack, J., Hinds, O., Yeo, B.T., Mohlberg, H., Amunts, K., Zilles, K., 2008. Cortical folding patterns and predicting cytoarchitecture. Cereb Cortex. 18**,** 1973-80.
Fjell, A.M., Westlye, L.T., Amlien, I., Espeseth, T., Reinvang, I., Raz, N., Agartz, I., Salat, D.H., Greve, D.N., Fischl, B., Dale, A.M., Walhovd, K.B., 2009. High consistency of regional cortical thinning in aging across multiple samples. Cereb Cortex. 19**,** 2001-12.
Fjell, A.M., Walhovd, K.B., 2010. Structural brain changes in aging: courses, causes and cognitive consequences. Rev Neurosci. 21**,** 187-221.
Folstein, M.F., Folstein, S.E., McHugh, P.R., 1975. "Mini-mental state". A practical method for grading the cognitive state of patients for the clinician. J Psychiatr Res. 12**,** 189-98.
Fornito, A., Whittle, S., Wood, S.J., Velakoulis, D., Pantelis, C., Yucel, M., 2006. The influence of sulcal variability on morphometry of the human anterior cingulate and paracingulate cortex. Neuroimage. 33**,** 843-54.
Fuster, J., 2008. The prefrontal cortex, Vol., Elsevier, London.
Fuster, J.M., 2001. The prefrontal cortex--an update: time is of the essence. Neuron. 30**,** 319-33.
Galantucci, S., Tartaglia, M.C., Wilson, S.M., Henry, M.L., Filippi, M., Agosta, F., Dronkers, N.F., Henry, R.G., Ogar, J.M., Miller, B.L., Gorno-Tempini, M.L., 2011. White matter damage in primary progressive aphasias: a diffusion tensor tractography study. Brain. 134**,** 3011-29.
Galton, C.J., Patterson, K., Graham, K., Lambon-Ralph, M.A., Williams, G., Antoun, N., Sahakian, B.J., Hodges, J.R., 2001. Differing patterns of temporal atrophy in Alzheimer's disease and semantic dementia. Neurology. 57**,** 216-25.
Genovese, C.R., Lazar, N.A., Nichols, T., 2002. Thresholding of statistical maps in functional neuroimaging using the false discovery rate. Neuroimage. 15**,** 870-8.
Gogtay, N., Giedd, J.N., Lusk, L., Hayashi, K.M., Greenstein, D., Vaituzis, A.C., Nugent, T.F., 3rd, Herman, D.H., Clasen, L.S., Toga, A.W., Rapoport, J.L., Thompson, P.M., 2004. Dynamic mapping of human cortical development during childhood through early adulthood. Proc Natl Acad Sci U S A. 101**,** 8174-9.
Goldman, P.S., 1979. Contralateral projections to the dorsal thalamus from frontal association cortex in the rhesus monkey. Brain Res. 166**,** 166-71.
Goncharova, II, Dickerson, B.C., Stoub, T.R., deToledo-Morrell, L., 2001. MRI of human entorhinal cortex: a reliable protocol for volumetric measurement. Neurobiol Aging. 22**,** 737-45.
Good, C.D., Johnsrude, I., Ashburner, J., Henson, R.N., Friston, K.J., Frackowiak, R.S., 2001a. Cerebral asymmetry and the effects of sex and handedness on brain structure: a voxel-based morphometric analysis of 465 normal adult human brains. Neuroimage. 14**,** 685-700.
Good, C.D., Johnsrude, I.S., Ashburner, J., Henson, R.N., Friston, K.J., Frackowiak, R.S., 2001b. A voxel-based morphometric study of ageing in 465 normal adult human brains. Neuroimage. 14**,** 21-36.
Gormezano, I., Grant, D.A., 1958. Progressive ambiguity in the attainment of concepts on the Wisconsin card sorting test. J Exp Psychol. 55**,** 621-7.
Gorno-Tempini, M.L., Rankin, K.P., Woolley, J.D., Rosen, H.J., Phengrasamy, L., Miller, B.L., 2004. Cognitive and behavioral profile in a case of right anterior temporal lobe neurodegeneration. Cortex. 40**,** 631-44.

Gorno-Tempini, M.L., Hillis, A.E., Weintraub, S., Kertesz, A., Mendez, M., Cappa, S.F., Ogar, J.M., Rohrer, J.D., Black, S., Boeve, B.F., Manes, F., Dronkers, N.F., Vandenberghe, R., Rascovsky, K., Patterson, K., Miller, B.L., Knopman, D.S., Hodges, J.R., Mesulam, M.M., Grossman, M., 2011. Classification of primary progressive aphasia and its variants. Neurology. 76**,** 1006-14.

Grieve, S.M., Clark, C.R., Williams, L.M., Peduto, A.J., Gordon, E., 2005. Preservation of limbic and paralimbic structures in aging. Hum Brain Mapp. 25**,** 391-401.

Grieve, S.M., Korgaonkar, M.S., Clark, C.R., Williams, L.M., 2011. Regional heterogeneity in limbic maturational changes: evidence from integrating cortical thickness, volumetric and diffusion tensor imaging measures. Neuroimage. 55**,** 868-79.

Grossman, M., McMillan, C., Moore, P., Ding, L., Glosser, G., Work, M., Gee, J., 2004. What's in a name: voxel-based morphometric analyses of MRI and naming difficulty in Alzheimer's disease, frontotemporal dementia and corticobasal degeneration. Brain. 127**,** 628-49.

Guenther, F.H., 2006. Cortical interactions underlying the production of speech sounds. J Commun Disord. 39**,** 350-65.

Gunturkun, O., 2011. The convergent evolution of neural substrates for cognition. Psychol Res.

Harlow, J.M., 1999. Passage of an iron rod through the head. 1848. J Neuropsychiatry Clin Neurosci. 11**,** 281-3.

Howard, M.A., Roberts, N., Garcia-Finana, M., Cowell, P.E., 2003. Volume estimation of prefrontal cortical subfields using MRI and stereology. Brain Res Brain Res Protoc. 10**,** 125-38.

Jack, C.R., Jr., Twomey, C.K., Zinsmeister, A.R., Sharbrough, F.W., Petersen, R.C., Cascino, G.D., 1989. Anterior temporal lobes and hippocampal formations: normative volumetric measurements from MR images in young adults. Radiology. 172**,** 549-54.

Jack, C.R., Jr., 1994. MRI-based hippocampal volume measurements in epilepsy. Epilepsia. 35 Suppl 6**,** S21-9.

Jenkinson, M., Smith, S., 2001. A global optimisation method for robust affine registration of brain images. Med Image Anal. 5**,** 143-56.

Jenkinson, M., Bannister, P., Brady, M., Smith, S., 2002. Improved optimization for the robust and accurate linear registration and motion correction of brain images. Neuroimage. 17**,** 825-41.

Kahn, I., Andrews-Hanna, J.R., Vincent, J.L., Snyder, A.Z., Buckner, R.L., 2008. Distinct cortical anatomy linked to subregions of the medial temporal lobe revealed by intrinsic functional connectivity. J Neurophysiol. 100**,** 129-39.

Kandel, E.R., Schwartz, J.H., Thomas, M.J., 2000. Principles of neural science Vol., McGraw-Hill, London

Kim, E.J., Sidhu, M., Gaus, S.E., Huang, E.J., Hof, P.R., Miller, B.L., Dearmond, S.J., Seeley, W.W., 2011. Selective Frontoinsular von Economo Neuron and Fork Cell Loss in Early Behavioral Variant Frontotemporal Dementia. Cereb Cortex.

Kipps, C.M., Davies, R.R., Mitchell, J., Kril, J.J., Halliday, G.M., Hodges, J.R., 2007. Clinical significance of lobar atrophy in frontotemporal dementia: application of an MRI visual rating scale. Dement Geriatr Cogn Disord. 23**,** 334-42.

Koikegami, H., Ozaki, N., 1967. Studies on the paralimbic brain structures. 3. On the nucleus accumbens and on the olfacto-tegmental tract in the Indian elephant. Acta Med Biol (Niigata). 15**,** 131-40.

Lambon Ralph, M.A., Cipolotti, L., Manes, F., Patterson, K., 2010. Taking both sides: do unilateral anterior temporal lobe lesions disrupt semantic memory? Brain. 133**,** 3243-55.

Levitt, J.J., Styner, M., Niethammer, M., Bouix, S., Koo, M.S., Voglmaier, M.M., Dickey, C.C., Niznikiewicz, M.A., Kikinis, R., McCarley, R.W., Shenton, M.E., 2009. Shape abnormalities of caudate nucleus in schizotypal personality disorder. Schizophr Res. 110**,** 127-39.

Lindberg, O., Ostberg, P., Zandbelt, B.B., Oberg, J., Zhang, Y., Andersen, C., Looi, J.C., Bogdanovic, N., Wahlund, L.O., 2009. Cortical morphometric subclassification of frontotemporal lobar degeneration. AJNR Am J Neuroradiol. 30**,** 1233-9.

Luppino, G., Matelli, M., Camarda, R.M., Gallese, V., Rizzolatti, G., 1991. Multiple representations of body movements in mesial area 6 and the adjacent cingulate cortex: an intracortical microstimulation study in the macaque monkey. J Comp Neurol. 311**,** 463-82.
Malykhin, N.V., Bouchard, T.P., Ogilvie, C.J., Coupland, N.J., Seres, P., Camicioli, R., 2007. Three-dimensional volumetric analysis and reconstruction of amygdala and hippocampal head, body and tail. Psychiatry Res. 155**,** 155-65.
McClelland, J.L., Rogers, T.T., 2003. The parallel distributed processing approach to semantic cognition. Nat Rev Neurosci. 4**,** 310-22.
McCormick, L.M., Ziebell, S., Nopoulos, P., Cassell, M., Andreasen, N.C., Brumm, M., 2006. Anterior cingulate cortex: an MRI-based parcellation method. Neuroimage. 32**,** 1167-75.
McEvoy, L.K., Holland, D., Hagler, D.J., Jr., Fennema-Notestine, C., Brewer, J.B., Dale, A.M., 2011. Mild cognitive impairment: baseline and longitudinal structural MR imaging measures improve predictive prognosis. Radiology. 259**,** 834-43.
McGinnis, S.M., Brickhouse, M., Pascual, B., Dickerson, B.C., 2011. Age-related changes in the thickness of cortical zones in humans. Brain Topogr. 24**,** 279-91.
McRobbie, D., Moore E, Graves, J., MR, P., 2005. MRI from Picture to Proton, Vol., University Press, Cambridge.
Mesulam, M.M., 1998. From sensation to cognition. Brain. 121 (Pt 6)**,** 1013-52.
Miller, B.L., Chang, L., Mena, I., Boone, K., Lesser, I.M., 1993. Progressive right frontotemporal degeneration: clinical, neuropsychological and SPECT characteristics. Dementia. 4**,** 204-13.
Neary, D., Snowden, J.S., Gustafson, L., Passant, U., Stuss, D., Black, S., Freedman, M., Kertesz, A., Robert, P.H., Albert, M., Boone, K., Miller, B.L., Cummings, J., Benson, D.F., 1998. Frontotemporal lobar degeneration: a consensus on clinical diagnostic criteria. Neurology. 51**,** 1546-54.
Ongur, D., Price, J.L., 2000. The organization of networks within the orbital and medial prefrontal cortex of rats, monkeys and humans. Cereb Cortex. 10**,** 206-19.
Ono, M., Kubik, S., CD, A., 1990. Atlas of cerebral sulci, Vol., Thieme, Stuttgart.
Patterson, K., Nestor, P.J., Rogers, T.T., 2007. Where do you know what you know? The representation of semantic knowledge in the human brain. Nat Rev Neurosci. 8**,** 976-87.
Pearson, R.C., Esiri, M.M., Hiorns, R.W., Wilcock, G.K., Powell, T.P., 1985. Anatomical correlates of the distribution of the pathological changes in the neocortex in Alzheimer disease. Proc Natl Acad Sci U S A. 82**,** 4531-4.
Perry, R.J., Graham, A., Williams, G., Rosen, H., Erzinclioglu, S., Weiner, M., Miller, B., Hodges, J., 2006. Patterns of frontal lobe atrophy in frontotemporal dementia: a volumetric MRI study. Dement Geriatr Cogn Disord. 22**,** 278-87.
Petrides, M., 2005. Lateral prefrontal cortex: architectonic and functional organization. Philos Trans R Soc Lond B Biol Sci. 360**,** 781-95.
Petrides, M., Tomaiuolo, F., Yeterian, E.H., Pandya, D.N., 2011. The prefrontal cortex: Comparative architectonic organization in the human and the macaque monkey brains. Cortex.
Price, C.J., Crinion, J.T., Macsweeney, M., 2011. A Generative Model of Speech Production in Broca's and Wernicke's Areas. Front Psychol. 2**,** 237.
Price, J.L., Drevets, W.C., 2010. Neurocircuitry of mood disorders. Neuropsychopharmacology. 35**,** 192-216.
Rabinovici, G.D., Jagust, W.J., Furst, A.J., Ogar, J.M., Racine, C.A., Mormino, E.C., O'Neil, J.P., Lal, R.A., Dronkers, N.F., Miller, B.L., Gorno-Tempini, M.L., 2008. Abeta amyloid and glucose metabolism in three variants of primary progressive aphasia. Ann Neurol. 64**,** 388-401.
Rabinovici, G.D., Miller, B.L., 2010. Frontotemporal lobar degeneration: epidemiology, pathophysiology, diagnosis and management. CNS Drugs. 24**,** 375-98.
Rankin, K.P., Salazar, A., Gorno-Tempini, M.L., Sollberger, M., Wilson, S.M., Pavlic, D., Stanley, C.M., Glenn, S., Weiner, M.W., Miller, B.L., 2009. Detecting sarcasm from paralinguistic cues: anatomic and cognitive correlates in neurodegenerative disease. Neuroimage. 47**,** 2005-15.

Ratiu, P., Talos, I.F., 2004. Images in clinical medicine. The tale of Phineas Gage, digitally remastered. N Engl J Med. 351**,** e21.
Raz, N., Gunning-Dixon, F., Head, D., Rodrigue, K.M., Williamson, A., Acker, J.D., 2004. Aging, sexual dimorphism, and hemispheric asymmetry of the cerebral cortex: replicability of regional differences in volume. Neurobiol Aging. 25**,** 377-96.
Raz, N., Lindenberger, U., Rodrigue, K.M., Kennedy, K.M., Head, D., Williamson, A., Dahle, C., Gerstorf, D., Acker, J.D., 2005. Regional brain changes in aging healthy adults: general trends, individual differences and modifiers. Cereb Cortex. 15**,** 1676-89.
Raz, N., Rodrigue, K.M., 2006. Differential aging of the brain: patterns, cognitive correlates and modifiers. Neurosci Biobehav Rev. 30**,** 730-48.
Raz, N., Rodrigue, K.M., Kennedy, K.M., Acker, J.D., 2007. Vascular health and longitudinal changes in brain and cognition in middle-aged and older adults. Neuropsychology. 21**,** 149-57.
Raz, N., Ghisletta, P., Rodrigue, K.M., Kennedy, K.M., Lindenberger, U., 2010. Trajectories of brain aging in middle-aged and older adults: regional and individual differences. Neuroimage. 51**,** 501-11.
Ronnback, A., Sagelius, H., Bergstedt, K.D., Naslund, J., Westermark, G.T., Winblad, B., Graff, C., 2011. Amyloid neuropathology in the single Arctic APP transgenic model affects interconnected brain regions. Neurobiol Aging.
Rosen, H.J., Allison, S.C., Schauer, G.F., Gorno-Tempini, M.L., Weiner, M.W., Miller, B.L., 2005. Neuroanatomical correlates of behavioural disorders in dementia. Brain. 128**,** 2612-25.
Saleem, K.S., Kondo, H., Price, J.L., 2008. Complementary circuits connecting the orbital and medial prefrontal networks with the temporal, insular, and opercular cortex in the macaque monkey. J Comp Neurol. 506**,** 659-93.
Scheibel, M.E., Scheibel, A.B., 1967. Structural organization of nonspecific thalamic nuclei and their projection toward cortex. Brain Res. 6**,** 60-94.
Schleicher, A., Zilles, K., Wree, A., 1986. A quantitative approach to cytoarchitectonics: software and hardware aspects of a system for the evaluation and analysis of structural inhomogeneities in nervous tissue. Journal of neuroscience methods. 18**,** 221-35.
Schleicher, A., Zilles, K., 1990. A quantitative approach to cytoarchitectonics: analysis of structural inhomogeneities in nervous tissue using an image analyser. Journal of microscopy. 157**,** 367-81.
Seeley, W.W., Bauer, A.M., Miller, B.L., Gorno-Tempini, M.L., Kramer, J.H., Weiner, M., Rosen, H.J., 2005. The natural history of temporal variant frontotemporal dementia. Neurology. 64**,** 1384-90.
Seeley, W.W., Crawford, R.K., Zhou, J., Miller, B.L., Greicius, M.D., 2009. Neurodegenerative diseases target large-scale human brain networks. Neuron. 62**,** 42-52.
Shany-Ur, T., Rankin, K.P., 2011. Personality and social cognition in neurodegenerative disease. Curr Opin Neurol. 24**,** 550-5.
Shaw, P., Kabani, N.J., Lerch, J.P., Eckstrand, K., Lenroot, R., Gogtay, N., Greenstein, D., Clasen, L., Evans, A., Rapoport, J.L., Giedd, J.N., Wise, S.P., 2008. Neurodevelopmental trajectories of the human cerebral cortex. J Neurosci. 28**,** 3586-94.
Shrout, P.E., Fleiss, J.L., 1979. Intraclass correlations: uses in assessing rater reliability. Psychol Bull. 86**,** 420-8.
Skipper, L.M., Ross, L.A., Olson, I.R., 2011. Sensory and semantic category subdivisions within the anterior temporal lobes. Neuropsychologia. 49**,** 3419-29.
Smith, S.M., 2002. Fast robust automated brain extraction. Hum Brain Mapp. 17**,** 143-55.
Smith, S.M., Jenkinson, M., Woolrich, M.W., Beckmann, C.F., Behrens, T.E., Johansen-Berg, H., Bannister, P.R., De Luca, M., Drobnjak, I., Flitney, D.E., Niazy, R.K., Saunders, J., Vickers, J., Zhang, Y., De Stefano, N., Brady, J.M., Matthews, P.M., 2004. Advances in functional and structural MR image analysis and implementation as FSL. Neuroimage. 23 Suppl 1**,** S208-19.

Sowell, E.R., Thompson, P.M., Tessner, K.D., Toga, A.W., 2001. Mapping continued brain growth and gray matter density reduction in dorsal frontal cortex: Inverse relationships during postadolescent brain maturation. J Neurosci. 21**,** 8819-29.
Steiger, J., 1980. Tests for comparing elements of a correlation matrix. Psychol Bull. 87**,** 245-51.
Stinear, C.M., Coxon, J.P., Byblow, W.D., 2009. Primary motor cortex and movement prevention: where Stop meets Go. Neurosci Biobehav Rev. 33**,** 662-73.
Stuss, D.T., Benson, D.F., 1984. Neuropsychological studies of the frontal lobes. Psychol Bull. 95**,** 3-28.
Stuss, D.T., Alexander, M.P., 2007. Is there a dysexecutive syndrome? Philos Trans R Soc Lond B Biol Sci. 362**,** 901-15.
Stuss, D.T., 2011. Functions of the frontal lobes: relation to executive functions. J Int Neuropsychol Soc. 17**,** 759-65.
Styner, M., Lieberman, J.A., Pantazis, D., Gerig, G., 2004. Boundary and medial shape analysis of the hippocampus in schizophrenia. Med Image Anal. 8**,** 197-203.
Styner, M., Oguz, I., Xu, S., Brechbuhler, C., Pantazis, D., Levitt, J.J., Shenton, M.E., Gerig, G., 2006. Framework for the Statistical Shape Analysis of Brain Structures using SPHARM-PDM. Insight J. 242-250.
Styner, M., Oguz, I., Xu, S., Pantazis, D., Gerig, G., 2007. Statistical group differences in anatomical shape analysis using the Hotelling T2 metric. Medical Imaging. 65123.
Suzuki, M., Zhou, S.Y., Takahashi, T., Hagino, H., Kawasaki, Y., Niu, L., Matsui, M., Seto, H., Kurachi, M., 2005. Differential contributions of prefrontal and temporolimbic pathology to mechanisms of psychosis. Brain. 128**,** 2109-22.
Tanev, K., Sablosky, M., Vento, J., O'Hanlon, D., 2011. Structural and functional neuroimaging methods in the diagnosis of dementias: A retrospective chart and brain imaging review. Neurocase.
Tartaglia, M.C., Rosen, H.J., Miller, B.L., 2011. Neuroimaging in dementia. Neurotherapeutics. 8**,** 82-92.
Teive, H.A., Munhoz, R.P., Caramelli, P., 2011. Historical aphasia cases: "Tan-tan", "Vot-vot", and "Cre nom!". Arq Neuropsiquiatr. 69**,** 555-8.
Thiebaut de Schotten, M., Ffytche, D.H., Bizzi, A., Dell'Acqua, F., Allin, M., Walshe, M., Murray, R., Williams, S.C., Murphy, D.G., Catani, M., 2011. Atlasing location, asymmetry and inter-subject variability of white matter tracts in the human brain with MR diffusion tractography. Neuroimage. 54**,** 49-59.
Tisserand, D.J., Pruessner, J.C., Sanz Arigita, E.J., van Boxtel, M.P., Evans, A.C., Jolles, J., Uylings, H.B., 2002. Regional frontal cortical volumes decrease differentially in aging: an MRI study to compare volumetric approaches and voxel-based morphometry. Neuroimage. 17**,** 657-69.
Toga, A.W., Thompson, P.M., Sowell, E.R., 2006. Mapping brain maturation. Trends Neurosci. 29**,** 148-59.
Wahlund, L.O., Pihlstrand, E., Jonhagen, M.E., 2003. Mild cognitive impairment: experience from a memory clinic. Acta Neurol Scand Suppl. 179**,** 21-4.
Walhovd, K.B., Westlye, L.T., Amlien, I., Espeseth, T., Reinvang, I., Raz, N., Agartz, I., Salat, D.H., Greve, D.N., Fischl, B., Dale, A.M., Fjell, A.M., 2011. Consistent neuroanatomical age-related volume differences across multiple samples. Neurobiol Aging. 32**,** 916-32.
Van Leemput, K., Bakkour, A., Benner, T., Wiggins, G., Wald, L.L., Augustinack, J., Dickerson, B.C., Golland, P., Fischl, B., 2009. Automated segmentation of hippocampal subfields from ultra-high resolution in vivo MRI. Hippocampus. 19**,** 549-57.
Welker, W.I., Seidenstein, S., 1959. Somatic sensory representation in the cerebral cortex of the racoon (Procyon lotor). J Comp Neurol. 111**,** 469-501.
Westlye, L.T., Walhovd, K.B., Dale, A.M., Bjornerud, A., Due-Tonnessen, P., Engvig, A., Grydeland, H., Tamnes, C.K., Ostby, Y., Fjell, A.M., 2010a. Life-span changes of the human brain white matter: diffusion tensor imaging (DTI) and volumetry. Cereb Cortex. 20**,** 2055-68.
Westlye, L.T., Walhovd, K.B., Dale, A.M., Bjornerud, A., Due-Tonnessen, P., Engvig, A., Grydeland, H., Tamnes, C.K., Ostby, Y., Fjell, A.M., 2010b. Differentiating

maturational and aging-related changes of the cerebral cortex by use of thickness and signal intensity. Neuroimage. 52**,** 172-85.
Whitwell, J.L., Jack, C.R., Jr., 2005. Comparisons between Alzheimer disease, frontotemporal lobar degeneration, and normal aging with brain mapping. Top Magn Reson Imaging. 16**,** 409-25.
Whitwell, J.L., Weigand, S.D., Gunter, J.L., Boeve, B.F., Rademakers, R., Baker, M., Knopman, D.S., Wszolek, Z.K., Petersen, R.C., Jack, C.R., Jr., Josephs, K.A., 2011. Trajectories of brain and hippocampal atrophy in FTD with mutations in MAPT or GRN. Neurology. 77**,** 393-8.
WHO, 1992. ICD-10 Classifications of Mental and Behavioural Disorder: Clinical Descriptions and Diagnostic Guidelines., Vol., Geneva.
Wilson, S.M., Ogar, J.M., Laluz, V., Growdon, M., Jang, J., Glenn, S., Miller, B.L., Weiner, M.W., Gorno-Tempini, M.L., 2009. Automated MRI-based classification of primary progressive aphasia variants. Neuroimage. 47**,** 1558-67.
Wilson, S.M., Dronkers, N.F., Ogar, J.M., Jang, J., Growdon, M.E., Agosta, F., Henry, M.L., Miller, B.L., Gorno-Tempini, M.L., 2010a. Neural correlates of syntactic processing in the nonfluent variant of primary progressive aphasia. J Neurosci. 30**,** 16845-54.
Wilson, S.M., Henry, M.L., Besbris, M., Ogar, J.M., Dronkers, N.F., Jarrold, W., Miller, B.L., Gorno-Tempini, M.L., 2010b. Connected speech production in three variants of primary progressive aphasia. Brain. 133**,** 2069-88.
Vincent, J.L., Kahn, I., Snyder, A.Z., Raichle, M.E., Buckner, R.L., 2008. Evidence for a frontoparietal control system revealed by intrinsic functional connectivity. J Neurophysiol. 100**,** 3328-42.
Viskontas, I.V., Possin, K.L., Miller, B.L., 2007. Symptoms of frontotemporal dementia provide insights into orbitofrontal cortex function and social behavior. Ann N Y Acad Sci. 1121**,** 528-45.
Wood, J.N., Grafman, J., 2003. Human prefrontal cortex: processing and representational perspectives. Nat Rev Neurosci. 4**,** 139-47.
Zhang, Y., Brady, M., Smith, S., 2001. Segmentation of brain MR images through a hidden Markov random field model and the expectation-maximization algorithm. IEEE Trans Med Imaging. 20**,** 45-57.
Zhang, Y., Qiu, C., Lindberg, O., Bronge, L., Aspelin, P., Backman, L., Fratiglioni, L., Wahlund, L.O., 2010. Acceleration of hippocampal atrophy in a non-demented elderly population: the SNAC-K study. Int Psychogeriatr. 22**,** 14-25.

11 APPENDIX

11.1 CLINICAL SYMPTOMS

Alexia: A general term for acquired reading disorders due to brain damage.

Apraxia of Speech: (AOS) is a motor speech disorder affecting an individual's ability to execute coordinated articulatory movements in the absence of muscular weakness. It is characterized especially by sound substitution errors, most often in phonetically complex words, by irregular articulatory breakdowns, articulatory "groping" and distortion of individual speech sounds. Like other apraxias, it only affects volitional movement patterns, and overlearned or "automatic" speech sequences may be uttered fluently. Apraxia of speech exists in developmental and acquired forms, the latter of which is common in stroke patients; it may also be an early and prominent symptom of **progressive nonfluent aphasia**.

Comportment: the manner in which one behaves or conducts oneself.

Prosopagnosia (Greek: "prosopon" = "face", "agnosia" = "not knowing") is a disorder of face perception where the ability to recognize faces is impaired, while the ability to recognize other objects may be relatively intact. One specific brain area that has been associated with prosopagnosia is the fusiform gyrus. Prosopagnosia may be an early (and?)prominent sign of **semantic dementia**.

Associative agnosia: A disorder of perception characterised by impaired recognition of physical objects despite preserved ability to apprehend their shape, as evidenced by e.g. copy drawing. It is considered a sign of **semantic dementia** but may occur in various brain lesions as a modality-specific deficit.

Surface alexia: A reading disorder characterized by impaired pronunciation of words with atypical sound-spelling correspondences often resulting in "phonetic" readings. In contrast, pseudowords such as *wug* and words with typical sound-spelling correspondences are read appropriately. Surface alexia occurs with various brain lesions but is characteristic of **semantic dementia**.

Agraphia: a loss of the ability to write or to express thoughts in writing because of a brain lesion. http://www.thefreedictionary.com/agraphia.

Surface agraphia (also **lexical agraphia** or **orthographic agraphia):** A writing disorder characterized by impaired spelling of words with atypical spelling-sound correspondences often resulting in "phonetic" spellings. In contrast, pseudowords such as *wug* and words with typical spelling-sound correspondences are spelled appropriately. Surface agraphia occurs with various brain lesions but is characteristic of **semantic dementia**.

11.2 VOLUMETRIC PROTOCOLS FOR UNPUBLISHED DATA

The subcallosal medial prefrontal cortex was traced in coronal orientation. Anterior border was the first slice in which the callosal white matter connects the two hemispheres and the posterior border was the last slice in which the inferior part of corpus callosum could be visualized. Between these landmarks all grey matter on the ventromedial surface was included. Intraclass correlation coefficient (ICC) was calculated to estimate the reliability of measurements. ICC was estimated on two occasions on 10 repeated measurements and was on both occasions above 0.91. Tracings of other frontal regions were done following Suzuki et al (Suzuki et al., 2005). For dorsolateral prefrontal cortex we summarized the grey matter volume of the superior frontal gyrus with grey matter volume of the middle frontal gyrus. ICC for other cortical regions has been reported previously (Lindberg et al., 2009).